

# Consistent clustering using $\ell_1$ fusion penalty

BY PETER RADCHENKO AND GOURAB MUKHERJEE

*Department of Data Sciences and Operations, University of Southern California,*

*Los Angeles, CA 90089-0809.*

radchenk@usc.edu    gourab@usc.edu

## SUMMARY

We study a convex regularized clustering framework that minimizes the within cluster sum of squares under an  $\ell_1$  fusion constraint on the cluster centroids. We track the entire solution path through a regularization path algorithm. Analyzing the associated population clustering procedure, we provide new insights on how the  $\ell_1$  fusion regularization incrementally induces partitions in the sample space. Based on these new perspectives, we propose a refined path algorithm, which in large samples can consistently detect the number of clusters and the associated partition of the space. Our method of analysis is fairly general and works for a wide range of population densities. Explicit characterization of the consistency conditions is provided for the case of Gaussian mixtures. On simulated data sets, we compare the performance of our method with a number of existing cluster estimation and modality assessment algorithms, and obtain encouraging results. We also demonstrate the applicability of our clustering approach for the detection of cellular subpopulations in a single-cell protein expression based virology study.

*Some key words:* Consistency; Number of Clusters; Convex Clustering; Fusion Penalties; Class discovery; Gaussian Mixture Models; Multi-modality;

## 1. INTRODUCTION

Clustering is one of the most popular statistical techniques for unsupervised classification and taxonomy detection (Hartigan, 1975; Kaufman & Rousseeuw, 2009). One limitation of the traditional methods, such as  $k$ -means, is the non-convexity of the corresponding optimization problems. However, several convex clustering algorithms have been proposed in recent years (Xu et al., 2004; Bach & Harchaoui, 2008; Chi & Lange, 2013). The speed and scalability of these algorithms makes them increasingly popular for cluster analysis of modern massive datasets. These algorithms are convex relaxations of the traditional non-convex clustering criteria, however, they do not naturally inherit the statistical consistency properties associated with the traditional methods. Here we study one such popular convex clustering framework, which is based on an  $\ell_1$  fusion penalty (Hocking et al., 2011), and show that in large samples it can consistently recover the true population sub-groups.

Consider the problem of clustering  $n$  observations,  $\mathbf{x}_1, \dots, \mathbf{x}_n$ , which are sampled from a Euclidean space,  $\mathbb{R}^p$ . The well-studied  $k$ -means approach (MacQueen et al., 1967; Hartigan, 1978; Pollard, 1981, 1982; Jain, 2010) proceeds by minimizing the within cluster sum of squares,  $\sum_{i=1}^n \|\mathbf{x}_i - \boldsymbol{\alpha}_i\|_2^2$ , with respect to the cluster centroids,  $\boldsymbol{\alpha}_1, \dots, \boldsymbol{\alpha}_n$ , under the restriction that the number of distinct cluster centroids is at most  $k$ . This restriction can be viewed as an  $\ell_0$  constraint on the centroids. Motivated by the Lasso and its variants (Tibshirani, 1996; Chen et al., 1998; Yuan & Lin, 2006; Tibshirani et al., 2005), which successfully use the  $\ell_1$  constraint as a surrogate

for the NP-hard  $\ell_0$  constraint, Hocking et al. (2011) consider the following  $\ell_1$  relaxation of the  $k$ -means clustering criterion:

$$\min_{\alpha_1, \dots, \alpha_n} \sum_{i=1}^n \|\mathbf{x}_i - \alpha_i\|_2^2 \quad \text{subject to} \quad \sum_{1 \leq i < j \leq n} \|\alpha_i - \alpha_j\|_1 \leq t. \quad (1)$$

When  $t = 0$ , the  $\ell_1$  penalty fuses all the cluster centroids together. Thus, all the observations are placed in the same cluster. When  $t \geq \sum_{i < j} \|\mathbf{x}_i - \mathbf{x}_j\|_1$ , we have  $\alpha_i = \mathbf{x}_i$  for all  $i$ , and thus, each observation forms its own cluster. Varying  $t$  between the two extremes creates a path of solutions to the regularized clustering problem.

Note that the objective criterion in (1) is convex and separable across dimensions. Consequently, the corresponding optimization problem reduces to independently minimizing  $p$  univariate convex clustering criteria. The univariate criterion in the Lagrangian form is given by:

$$\min_{\alpha_1, \dots, \alpha_n} \sum_{i=1}^n (x_i - \alpha_i)^2 + \lambda \sum_{1 \leq i < j \leq n} |\alpha_i - \alpha_j|, \quad (2)$$

where the penalty parameter  $\lambda$  varies from 0 to  $\infty$ . In this paper we focus on the analysis of the univariate clustering criterion (2).

Recently, algorithms with appealing computational properties have been proposed to solve various modified versions of the clustering criterion (2), such as those using weights or  $\ell_2$  regularization. Hocking et al. (2011), Chi & Lange (2013) and the references therein provide specific examples. Here we take a different perspective and study the statistical accuracy with which a solution to (2), computed on a random sample, can recover the true population clusters. We also show that the solution path can be used to recover the correct number of clusters and compare it with traditional *number of clusters* estimation techniques (Milligan & Cooper, 1985; Tibshirani et al., 2001). Our results provide support for the use of  $\ell_1$  fusion penalties in clustering.

The  $\ell_1$  penalty, which is extensively used for variable selection (Tibshirani, 2011), also finds its use in trend filtering (Tibshirani, 2013) and high-dimensional clustering problems (Soltanolkotabi & Candés, 2012; Witten & Tibshirani, 2010). Another related approach, the fused Lasso (Rinaldo et al., 2009; Tibshirani & Walther, 2005; Hoefling, 2010), deals with applications having ordered features and checks for local constancy of their associated coefficients. This approach penalizes the successive differences of the coefficients. Shen & Huang (2010); Shen et al. (2012); Ke et al. (2013); Bondell & Reich (2008) have proposed methods based on fusion penalties, which apply to all the pairwise differences of coefficients. These approaches can successfully recover the grouping structure of predictors in a high-dimensional regression setup. However, the theory developed for these methods focusses on the homogeneity of regression coefficients and cannot be used in the unsupervised clustering setup considered in this paper.

The paper is organized as follows. In Section 2 we develop an efficient *merging algorithm* for producing a piecewise linear regularization path of solutions to the clustering criterion (2). In order to understand the large sample behaviour of the solution path we introduce an equivalent *splitting procedure*, which can recover all the corresponding cluster splits by solving a sequence of optimization problems. An analysis of the population version of the splitting procedure reveals that an overwhelming majority of the cluster splits (and, thus, merges) are in some sense negligible. As a result, in Section 2 we introduce a key modification to the merging algorithm, and name the new approach the *Big Merge Tracker*. In Section 3 we provide general conditions for consistency of our procedure relative to its population analog. We then apply the general result to establish consistency in the case where the underlying distribution is unimodal (Section 3) and in the case it is a mixture of two Gaussians (Section 4). In Section 5 we conduct a detailed empirical

analysis of our approach. More specifically, we use simulated data to show strong performance of our method relative to popular existing approaches for assessing modality and estimating the number of clusters. We also illustrate the use of our method in analysis of single-cell virology datasets. The proofs for all the theoretical results are provided in the appendix.

## 2. A PATH ALGORITHM & ITS PROPERTIES AND REFINEMENTS

Note that a solution path could be produced using the highly general fused lasso algorithm in Hoefling (2010), however, below we obtain a very simple fitting procedure by analyzing our clustering criterion, (2), directly. The path algorithm we describe here is a bottom up procedure, which starts at  $\lambda = 0$ , with each observation forming its own cluster, and then gradually merges suitable clusters as  $\lambda$  increases. Fix  $\lambda$ , and suppose that  $C$  is one of the clusters identified by the solution to the optimization problem (2). Write  $\alpha_C$  for the centroid of cluster  $C$ , and denote the corresponding cluster average by  $\bar{X}_C$ . As pointed out in Hocking et al. (2011), the first order conditions for criterion (2) imply

$$\alpha_C = \bar{X}_C + \lambda \sum_{j, \alpha_j \neq \alpha_C} \text{sign}(\alpha_j - \alpha_C). \quad (3)$$

Note that until the cluster partition is modified, parameter  $\lambda$  is the only component on the right-hand side of the equation that can change. Thus, equation (3) provides a simple way of tracking the piecewise linear paths of the centroids  $\alpha_i$ . Another consequence of the first order conditions is the fact that as  $\lambda$  increases, the only way that the clusters get modified is some of them get merged together (Hocking et al., 2011). Hence, we can store the full cluster partition path by keeping track of the merges and the corresponding values of the tuning parameter  $\lambda$ . Algorithm 1 makes this idea precise, and Theorem 1 provides a rigorous justification.

INITIALIZE:

Sort data in ascending order and store them as  $\mathbf{x} = \{x_1, \dots, x_n\}$ .

Set  $K$ , the number of clusters, equal to  $n$ . For each  $i$  in  $1, \dots, n$ , set  $C_i = \{x_i\}$ .

REPEAT:

Find the adjacent centroid distances standardized by cluster sizes:

$$d(j, j+1) \leftarrow (\bar{X}_{C_{j+1}} - \bar{X}_{C_j}) / (|C_j| + |C_{j+1}|).$$

Find the clusters that minimize this distance:  $j^* \leftarrow \arg \min_j d(j, j+1)$ .

Merge the clusters that were found:  $C_{j^*} \leftarrow C_{j^*} \cup C_{j^*+1}$ .

Store the above merge and the corresponding  $\lambda$  value:  $\lambda = d(j^*, j^*+1)$ .

Relabel the remaining clusters: for  $j > j^*$  set  $C_j \leftarrow C_{j+1}$ .

Reduce the total number of clusters:  $K \leftarrow K - 1$ .

UNTIL  $K = 1$ .

OUTPUT: Sequence of cluster merges and corresponding  $\lambda$  values.

### Algorithm 1: Merging Algorithm

The following result shows that the above algorithm reproduces the sequence of cluster partitions and the corresponding  $\lambda$  values from the optimization problem (2). In the proof we also

verify that the sequence of  $\lambda$  values, corresponding to successive merges in Algorithm 1, is increasing.

**THEOREM 1.** *Suppose that the observations are generated from a continuous univariate distribution. Then, with probability one, the sequence of merges and corresponding  $\lambda$  values produced by the merging algorithm is the same as the sequence corresponding to the optimization criterion (2).*

For the theoretical analysis, it is helpful to recover the sequence of cluster partitions in a top down approach: we start with everything in one cluster and then split the clusters iteratively. We call a representation of the cluster  $C$  as  $C = C_1 \cup C_2$  a split partition or, simply, a split, if  $\max C_1 < \min C_2$ . Theorem 2 shows that the sequence of cluster splits corresponding to the optimization problem (2) is given by the *splitting procedure*, which is described in Algorithm 2.

**INITIALIZE:**

Sort data in ascending order and store them as  $\mathbf{x} = \{x_1, \dots, x_n\}$ .

Set the current partition of  $\mathbf{x}$  to  $\mathbf{x}$ .

**REPEAT:**

Select one cluster,  $C$ , with  $|C| > 1$ , from a current cluster partition of  $\mathbf{x}$ .

Find a split partition  $C = C_1 \cup C_2$ , that maximizes the distance  $\bar{X}_{C_2} - \bar{X}_{C_1}$ .

Store the split  $C = C_1 \cup C_2$  and the corresponding value  $\lambda = (\bar{X}_{C_2} - \bar{X}_{C_1}) / |C|$ .

Replace  $C$  with  $C_1 \cup C_2$  in the current partition of  $\mathbf{x}$ .

**UNTIL:** All the clusters in the current partition of  $\mathbf{x}$  are of size one.

**OUTPUT:** Sequence of cluster splits and corresponding  $\lambda$  values.

**Algorithm 2:** Splitting Procedure

**THEOREM 2.** *Suppose that the observations are generated from a continuous univariate distribution. Then, with probability one, the sequence of merges and corresponding  $\lambda$  values produced by the merging algorithm exactly matches the sequence of splits and the corresponding  $\lambda$  values produced by the splitting procedure.*

To understand the large sample behavior of the solution to the optimization problem (2), we will concentrate on the splitting procedure. It is reasonable to expect that, as  $n$  tends to infinity, the sequence of splits of the sample splitting procedure should be close to that of the splitting procedure defined on the population. The population splitting procedure can be defined by replacing the averages that appear in the sample procedure with the corresponding conditional means. To formalize the population splitting procedure, we will start with some definitions. For the remainder of the paper, we will make the following assumption about the underlying distribution, from which the observations are generated.

- The underlying distribution has a finite first moment and a real valued density,  $f$ .

*Population Splitting Procedure.* For concreteness, we will focus on the case where the support of the distribution is of the form  $D = (L_0, R_0)$ , where  $-\infty \leq L_0 < R_0 \leq \infty$ . Thus, every open interval in  $D$  contains positive probability. Given an interval  $(l, r)$ , which is allowed to have

infinite length, we write  $\mu_{l,r}$  for the population conditional mean on  $(l, r)$ :

$$\mu_{l,r} = \left( \int_l^r f(x) dx \right)^{-1} \int_l^r x f(x) dx. \quad (4)$$

We set  $\mu_{r,r} = r$ , by continuity. We also define  $\hat{\mu}_{l,r}$  as the corresponding sample average:

$$\hat{\mu}_{l,r} = \left( \sum_i 1_{\{l \leq x_i \leq r\}} \right)^{-1} \sum_i x_i 1_{\{l \leq x_i \leq r\}}. \quad (5)$$

Consider  $L$  and  $R$ , such that  $(L, R) \subseteq D$ . For  $a \in [L, R]$  we define

$$G_{L,R}(a) = \mu_{a,R} - \mu_{L,a}. \quad (6)$$

Note that  $G_{L,R}(L) = \mu_{L,R} - L$  and  $G_{L,R}(R) = R - \mu_{L,R}$ . We also define  $\hat{G}_{L,R}(a)$  as the empirical analog of  $G_{L,R}(a)$ , i.e.  $\hat{G}_{L,R}(a) = \hat{\mu}_{a,R} - \hat{\mu}_{L,a}$ .

The sample splitting procedure described above can be summarized as follows. Start with all observations in one cluster. Set  $L = \min_i x_i$  and  $R = \max_i x_i$ . Take any  $s$  in the set  $\arg \max \hat{G}_{L,R}$ . Note that  $s$  is guaranteed to be located strictly between two of the observations. Split the sample into two clusters: observations below  $s$  and those above  $s$ . Repeat the above splitting procedure on each of the new clusters. Continue splitting until all of the clusters are of size one.

The population analog uses  $G$  rather than  $\hat{G}$ . For each current pair of values  $L$  and  $R$ , the population splitting procedure finds  $s = \arg \max G_{L,R}$ , then partitions  $(L, R)$  into subintervals  $(L, s)$  and  $(s, R)$ , on which the procedure is repeated. If  $s$  is an interior point of  $(L, R)$ , then we call it a *split point*, and we call the corresponding partition a *split*. Otherwise, the procedure essentially wants to split off an endpoint; we call the corresponding operation a *truncation* rather than a split. If  $\arg \max G_{L,r} = r$  for all  $r \in (R^*, R]$ , then we truncate the interval  $(L, R)$  to the interval  $(L, R^*)$ . Analogously, if  $\arg \max G_{l,R} = l$  for all  $l \in [L, L^*)$ , we truncate  $(L, R)$  to  $(L^*, R)$ . If there exists a continuous non-decreasing function  $l \mapsto R_l$ , such that  $\arg \max G_{l,R_l} = \{l, R_l\}$ , for all  $l \in (L, L^*]$ , then we truncate  $(L, R)$  to the interval  $(L^*, R_{L^*})$ .

Consider Figure 1 for illustration of the population splitting procedure corresponding to a symmetric Gaussian mixture distribution,  $0.5 N(-2, 1) + 0.5 N(2, 1)$ . It contains four plots of  $G_{L,R}$ , corresponding to different choices of  $L$  and  $R$ . For all sufficiently large  $|L|$  and  $R$ , the maximum of  $G_{L,R}$  can only be achieved at the endpoints. Note that  $G_{L,R}(L) < G_{L,R}(R)$  when  $|L| < R$ , as illustrated by plot B. However, when  $R_L = |L|$  (plots A, C and D), we have  $G_{L,R_L}(L) = G_{L,R_L}(R_L) = |L|$ . Thus, the population splitting procedure continuously truncates the support of the distribution to  $(L, |L|)$ , as  $L$  is increased, until the maximum of  $G_{L,|L|}$  can be achieved at an interior point (plot C). Denote this point by  $s^*$ , and the corresponding left-most endpoint by  $L^*$ . Note that  $s^*$  is also a split point, as no further truncation of the support can be performed (plot D). Thus, the population splitting procedure truncates the support of the distribution to the interval  $(L^*, |L^*|)$ , then splits it into  $(L^*, s^*)$  and  $(s^*, |L^*|)$ .

For a non-symmetric Gaussian mixture, the population splitting procedure operates in a similar fashion (see Figure 5 in the Appendix B). However, the general equality  $G_{L,R_L}(L) = G_{L,R_L}(R_L)$  does not result in  $R_L = |L|$ , but instead simplifies to  $\mu_{L,R_L} = (L + R_L)/2$ .

*Key Modification to the Sample Clustering Procedure.* In the sample, the truncation operation corresponds to peeling a large number of tiny clusters off the ends of a large cluster. This correspondence is formalized by the results in the next section. For example, consider the situation

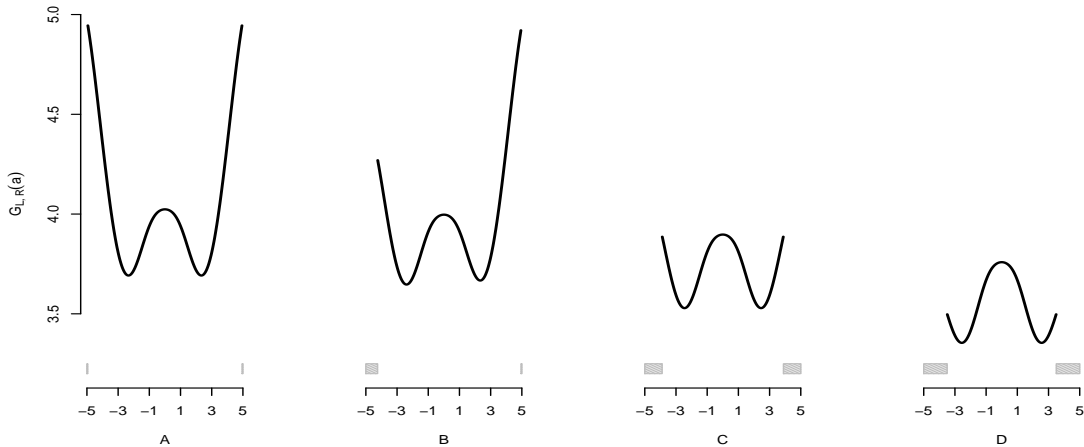


Fig. 1. An illustration of the population splitting procedure for the Gaussian mixture,  $0.5 N(-2, 1) + 0.5 N(2, 1)$ .

where the underlying distribution has a unimodal density, and take an arbitrarily small positive  $\epsilon$ . Corollary 1 in the next section implies that, with probability tending to one, each sample split peels off a cluster of size less than  $\epsilon n$ . It follows that when recording the sample splits we need to distinguish between those that correspond to splits in the population procedure and those that correspond to truncations. Based on this observation, we propose to modify the procedure in Algorithm 2 by only tracking the splits where both of the resulting clusters have significant sizes. More specifically, given a threshold  $\alpha$ , we only store the splits where the corresponding cluster sizes are above  $\alpha n$ . The rest of the splits are removed from the final output. We also replace the stored splits with the corresponding split points. The resulting sequence of split points can then be reinterpreted as a sequence of splits, or a sequence of merges, using the full sample. For example, if the final output contains no split points, then all of the observations in the sample are placed in the same cluster.

Figure 2 illustrates the path of Algorithm 1 on a sample of 1000 observations, generated independently from the symmetric Gaussian mixture distribution used in Figure 1. The scatter plot on the left displays the cluster proportions for each pair of clusters merged along the path. We found only one merge in which both cluster sizes pass the  $\alpha = 0.1$  threshold. The *big merge* occurs at a point where the current number of clusters is 32. Observations, together with cluster memberships before and after the split, are displayed on the two rightmost plots. The non-shaded points belong to clusters with non-appreciable size.

The equivalence between the splitting procedure and the merging algorithm implies that in the modification of Algorithm 1 we should only track the merges where both of the merging clusters have sizes above  $\alpha n$ . For any such merge, the corresponding split point is placed midway between the two closest representatives of the two clusters being merged. We call this modified approach the *Big Merge Tracker* (BMT) with threshold  $\alpha$ . In the next section we show that, under some regularity conditions, the sequence of split points identified by BMT converges to the sequence of split points in the population splitting procedure.

### 3. GENERAL CONSISTENCY RESULTS

We start with a few definitions. Take a small positive  $\delta$ . We will consider perturbations of the original population splitting procedure by allowing some small room, controlled by  $\delta$ , in the

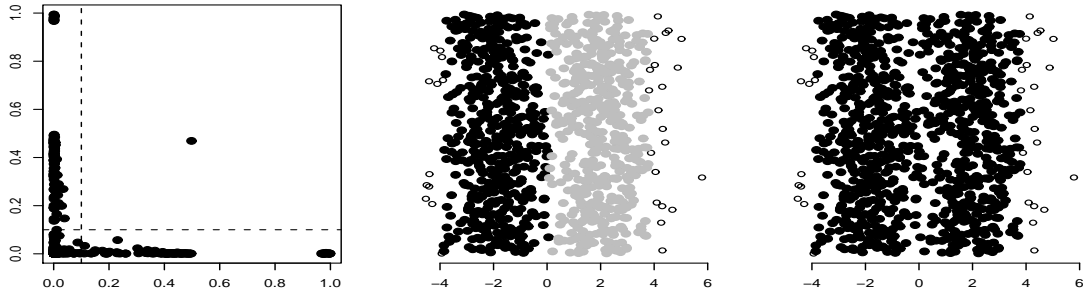


Fig. 2. The plots illustrate the path of Algorithm 1 on a sample of 1000 observations from a symmetric Gaussian mixture,  $0.5 N(-2, 1) + 0.5 N(2, 1)$ . The scatter plot on the left displays the cluster proportions for each pair of clusters merged along the hierarchical path. The next two plots show the cluster memberships before and after the *big merge*.

placement of the split points. Also, these modified procedures will have only splits, and no truncations. More specifically, given a current cluster,  $(L, R)$ , we allow the split point to be placed at any location  $s \in (L, R)$  that satisfies either  $\sup G_{L,R} - G_{L,R}(s) < \delta$  or  $|s| > \delta^{-1}$ . These modifications of the population splitting procedure will be referred to as  $\delta$ -precision procedures.

We will write  $P_{L,R}$  for the probability assigned to the interval  $(L, R)$  by the underlying distribution. If a split  $(L, R) = (L, s) \cup (s, R)$  has  $P_{L,s} > \alpha$  and  $P_{s,R} > \alpha$ , we will call it an  $\alpha$ -split. Suppose that the population splitting procedure produces  $k$  splits corresponding to the split points  $s_1, \dots, s_k$ . Let  $\alpha^* = \sup\{\alpha, \text{ all splits of the population procedure are } \alpha\text{-splits}\}$ . We will call the population splitting procedure *continuous* if for every positive  $\epsilon$  there exists a  $\delta$ , such that, when  $\alpha \in (\epsilon, \alpha^* - \epsilon)$ , the number of  $\alpha$ -splits in each  $\delta$ -precision procedure is exactly  $k$ , and, if  $k > 0$ , the corresponding split points  $\tilde{s}_1, \dots, \tilde{s}_k$  satisfy  $\max_l |\tilde{s}_l - s_l| < \epsilon$ . The next result demonstrates that if the population splitting procedure is continuous, then the split points of the Big Merge Tracker converge to their population counterparts.

**THEOREM 3.** *Suppose that the population splitting procedure is continuous. Consider a positive  $\alpha$ , such that every split of the population procedure is an  $\alpha$ -split. Then, the Big Merge Tracker with threshold  $\alpha$  identifies the same number of splits as the population splitting procedure, with probability tending to one as  $n$  goes to infinity. In addition, the corresponding BMT split points converge to their population counterparts in probability.*

We can establish continuity of the population splitting procedure by using the properties of the underlying distribution. For example, consider a unimodal distribution. More specifically, the density  $f$  is either strictly monotone on its support, or there exists a point  $c$  for which  $f$ , on its support, is strictly increasing to the left of  $c$  and strictly decreasing to the right of  $c$ . We can show that the corresponding population splitting procedure is continuous, which allows us to apply Theorem 3. The next result demonstrates that, with probability tending to one, the Big Merge Tracker produces no split points, and thus, places all the observations in the same cluster.

**COROLLARY 1.** *Suppose that the observations are generated from a unimodal distribution. Then, the population procedure produces no splits. Also, for each positive  $\alpha$ , the following statement holds with probability tending to one as  $n$  goes to infinity: Big Merge Tracker with threshold  $\alpha$  puts all the observations in the same cluster.*

Next, we apply Theorem 3 to characterize consistency of the Big Merge Tracker for Gaussian mixture distributions. Consistency analysis of the BMT for other parametric densities can be conducted in similar fashion.

#### 4. FURTHER RESULTS & ANALYSIS OF GAUSSIAN MIXTURE DISTRIBUTIONS

Suppose that  $L$  and  $R$  are the only two maxima of  $G_{L,R}$ , and consider the inequality

$$(R - L) [f(L) \vee f(R)] < P_{L,R}. \quad (7)$$

This inequality is important for the statement of Theorem 4, given below. In the proof of Theorem 4 we show that the above ensures balanced truncation, i.e. that the interval  $(L, R)$  is simultaneously truncated at both ends.

For concreteness and for the clarity of the exposition, we will focus on the case where  $f$  is a mixture of two distinct Gaussian densities on the real line. Define  $R_L = \max\{R : \mu_{L,R} = (L + R)/2\}$ . Under inequality (7), the population splitting procedure continuously truncates the support of the distribution to  $(L, R_L)$ , as  $L$  is increased, until the maximum of  $G_{L,R}$  can be achieved at an interior point. Define  $L^*$  as the smallest  $L$  for which there exists an  $s$  in  $(L, R_L)$ , such that  $\mu_{L,s} = (L + s)/2$  and  $\mu_{s,R_L} = (s + R_L)/2$ . Write  $s^*$  for the corresponding point  $s$ , and let  $R^*$  stand for  $R_{L^*}$ . In the proof of Theorem 4, stated below, we show that under (7) the support of the distribution is truncated to the interval  $(L^*, R^*)$ , which is then split at  $s^*$ .

Let  $\underline{m}$  denote the local minimum of  $f$ . For concreteness we will focus on the case  $s^* \leq \underline{m}$ . The case  $s^* > \underline{m}$  can be analyzed analogously. Denote by  $\bar{m}_2$  the right-most mode of  $f$  and by  $L^\diamond$  the reflection of  $R_{\underline{m}}$  across the point  $\bar{m}_2$ , i.e. let  $L^\diamond = 2\bar{m}_2 - R_{\underline{m}}$  (Figure 3). According to Corollary 1, to ensure there is no second split, it is enough to check that the left endpoint of the interval  $(s^*, R^*)$  is truncated all the way to  $\underline{m}$  without the maximum of  $G$  moving to an interior point. In the proof of Theorem 4 we show that this is indeed the case, provided inequality (7) holds for all  $L \in [s^*, L^\diamond]$  and  $R \in [R_{\underline{m}}, R^*]$ .

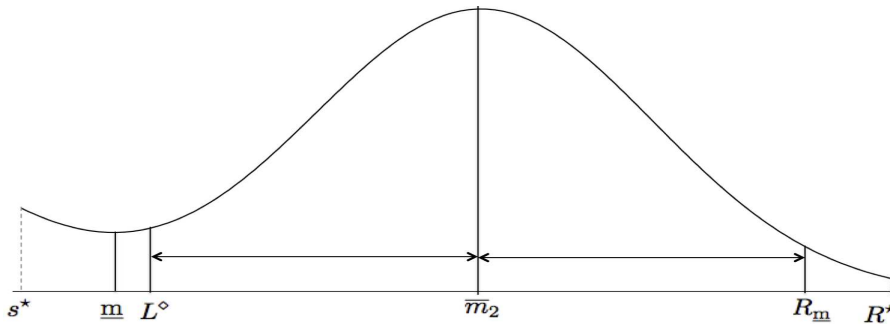


Fig. 3. The truncated density of  $0.4 N(-2, 1) + 0.6 N(2, 1)$  after the first split. There is no second split, because inequality (7) holds for all  $L \in [s^*, L^\diamond]$  and  $R \in [R_{\underline{m}}, R^*]$

The above discussion is formalized by the following result.

**THEOREM 4.** *Let  $f$  be a mixture of two Gaussian densities. Suppose that inequality (7) holds for all  $L \leq L^*$  and  $R \geq R^*$ . If (7) also holds for all  $L \in [s^*, L^\diamond]$  and  $R \in [R_{\underline{m}}, R^*]$ , then*

(i) *the population splitting procedure is continuous, and  $s^*$  is its only split point;*



- (ii) with probability tending to one, BMT with threshold  $\alpha < P_{L^*,s^*} \wedge P_{s^*,R^*}$  produces exactly one split point, which converges to  $s^*$  in probability.

Note that if the balanced truncation takes one of the end points all the way to  $\underline{m}$ , without producing an  $s^*$ , then, by Corollary 1, the population procedure produces no splits.

Next, we check the conditions of Theorem 4 for various mixtures of two Gaussian distributions on the real line. In Table 1, we document the behaviour of the population splitting procedure, and thus, the large sample performance of the Big Merge Tracker. For 7 different levels of separation between the two normal means we consider 9 different mixing proportions, from the symmetric case of 50 : 50 mixing to the highly non-symmetric 10 : 90 mixing. The behavior of the population splitting procedure in other cases can be interpolated from the table using continuity arguments. We present, where applicable, the location of the first split point,  $s^*$ , as well as the corresponding  $L^*$  and  $R^*$ . The local minimum of the density,  $\underline{m}$ , and the split point minimizing the expected misclassification error  $s_{MC}$ , are also provided. In all the cases where  $s^*$  is reported we verified the conditions of Theorem 4. Consequently, the conclusion of Theorem 4 is valid, and BMT produces two clusters, with the split point converging to  $s^*$  in probability. In the rest of the cases, we checked that condition (7) holds for all  $L \leq \underline{m}$  and all  $R > R_{\underline{m}}$ . This ensures that the balanced truncation takes  $L$  all the way to  $\underline{m}$ , and thus reduces the density to a unimodal one. Corollary 1 then implies that the population splitting procedure does not produce any splits. In summary, BMT is able to separate the two Gaussian distributions with probability tending to one, as long as the distance between the means is not too small, and the mixture is not too uneven.

*Computer Assisted Characterization.* Because analytical solutions are not available, we find  $L^*$ ,  $R^*$  and  $s^*$  numerically. It follows from the arguments in the proof of Theorem 4 that we only need to consider the values of  $L$  that satisfy  $2\bar{m}_1 - L \leq 2\bar{m}_2 - R_L$ , where  $\bar{m}_1 < \bar{m}_2$  are the two local maxima of  $f$ . For each given  $L$  we locate  $R_L$  using  $\mu_{L,R_L} = (L + R_L)/2$ . Then we focus on  $s$ , the local maximum of  $G_{L,R_L}$ , and compute  $\delta_1 = \mu_{L,s} - (L + s)/2$  and  $\delta_2 = \mu_{s,R_L} - (s + R_L)/2$ . Note that at  $L = L^*$  we have  $\delta_1 = \delta_2 = 0$ . Under inequality (7), we also have  $\delta_1 > 0$  and  $\delta_2 < 0$  for  $L < L^*$ . Thus, as  $L$  is increased,  $L^*$  can be taken as the first point where the deltas simultaneously change signs.

Closed form expressions for  $\mu_{L,R}$ ,  $G_{L,R}$  and  $G'_{L,R}$  are provided in Appendix B. Figure 5 in the Appendix B displays  $G_{L,R}(a)$ ,  $f$  and  $G'_{L,R}$  (normalized), corresponding to the  $0.35N(-4, 1) + 0.65N(4, 1)$  distribution, for three values of  $L$ : (a)  $L < L^*$ , (b)  $L = L^*$ , (c)  $L > L^*$ . Locations of  $\mu_{L,s}$ ,  $(L + s)/2$ ,  $\mu_{s,R_L}$  and  $(s + R_L)/2$  are also provided.

*Adjustment to the BMT.* When the separation between the Normal means is very small, the population splitting procedure can still be successful at finding a split point by massively truncating the support. In low sample sizes, this *zooming-in* effect may make BMT non-robust, as its effectiveness depends on the shape of the truncated empirical distribution. Studying the behaviour of the population splitting procedure on  $0.5N(-1.1, 1) + 0.5N(1.1, 1)$ , which is a very difficult example for bi-modality detection (see Section 5.1), we found  $|L^*| = R^* = 1.19$ , and the probability of  $(L^*, R^*)$  is  $\Phi(-1.19 - 1) + \Phi(-1.19 + 1) = 47.5\%$ . Based on the above, we propose an adjustment to the Big Merge Tracker. If the sum of proportions of the two merging clusters in the last big merge is less than 50%, we do not report any merges. Preventing the corresponding splitting procedure from truncating more than 50% of the data, while searching for the first split, slightly reduces its efficiency, but makes it more robust to sampling fluctuations.

Table 1. Finding splits for 2-normal mixtures:  $p_1 N(\mu_1, 1) + p_2 N(\mu_2, 1)$ 

CASE	$p_1$	$p_2$	$\mu_1$	$\mu_2$	$s_{MC}$	$\underline{m}$	$s^*$	$L^*$	$R^*$	2nd split
$ \mu_2 - \mu_1  = 9$	0.50	0.50	-4.50	4.50	0.00	0.00	0.00	-8.99	8.99	NO
	0.45	0.55	-4.50	4.50	-0.02	-0.02	-0.45	-8.53	9.43	NO
	0.40	0.60	-4.50	4.50	-0.04	-0.05	-0.90	-8.08	9.88	NO
	0.35	0.65	-4.50	4.50	-0.07	-0.07	-1.36	-7.62	10.33	NO
	0.30	0.70	-4.50	4.50	-0.09	-0.10	-1.82	-7.17	10.79	NO
	0.25	0.75	-4.50	4.50	-0.12	-0.13	-2.31	-6.67	11.24	NO
	0.20	0.80	-4.50	4.50	-0.15	-0.16	-2.90	-6.09	11.70	NO
	0.15	0.85	-4.50	4.50	-0.19	-0.20	-3.82	-5.09	12.16	NO
	0.10	0.90	-4.50	4.50	-0.24	-0.26	NO			
$ \mu_2 - \mu_1  = 8$	0.50	0.50	-4.00	4.00	0.00	0.00	0.00	-7.99	7.99	NO
	0.45	0.55	-4.00	4.00	-0.03	-0.03	-0.40	-7.58	8.38	NO
	0.40	0.60	-4.00	4.00	-0.05	-0.05	-0.80	-7.17	8.78	NO
	0.35	0.65	-4.00	4.00	-0.08	-0.08	-1.22	-6.77	9.19	NO
	0.30	0.70	-4.00	4.00	-0.11	-0.11	-1.64	-6.34	9.59	NO
	0.25	0.75	-4.00	4.00	-0.14	-0.15	-2.12	-5.86	9.99	NO
	0.20	0.80	-4.00	4.00	-0.17	-0.18	-2.72	-5.25	10.40	NO
	0.15	0.85	-4.00	4.00	-0.22	-0.23	NO			
	0.10	0.90	-4.00	4.00	-0.28	-0.29	NO			
$ \mu_2 - \mu_1  = 7$	0.50	0.50	-3.50	3.50	0.00	0.00	0.00	-6.98	6.98	NO
	0.45	0.55	-3.50	3.50	-0.03	-0.03	-0.35	-6.63	7.34	NO
	0.40	0.60	-3.50	3.50	-0.06	-0.06	-0.71	-6.27	7.69	NO
	0.35	0.65	-3.50	3.50	-0.09	-0.10	-1.09	-5.90	8.04	NO
	0.30	0.70	-3.50	3.50	-0.12	-0.13	-1.49	-5.49	8.39	NO
	0.25	0.75	-3.50	3.50	-0.16	-0.17	-1.97	-5.01	8.75	NO
	0.20	0.80	-3.50	3.50	-0.20	-0.22	-2.66	-4.32	9.12	NO
	0.15	0.85	-3.50	3.50	-0.25	-0.27	NO			
	0.10	0.90	-3.50	3.50	-0.31	-0.34	NO			
$ \mu_2 - \mu_1  = 6$	0.50	0.50	-3.00	3.00	0.00	0.00	0.00	-5.99	5.99	NO
	0.45	0.55	-3.00	3.00	-0.03	-0.04	-0.32	-5.66	6.28	NO
	0.40	0.60	-3.00	3.00	-0.07	-0.08	-0.64	-5.34	6.59	NO
	0.35	0.65	-3.00	3.00	-0.10	-0.12	-0.99	-4.99	6.89	NO
	0.30	0.70	-3.00	3.00	-0.14	-0.16	-1.39	-4.59	7.20	NO
	0.25	0.75	-3.00	3.00	-0.18	-0.21	-1.91	-4.07	7.52	NO
	0.20	0.80	-3.00	3.00	-0.23	-0.26	NO			
	0.15	0.85	-3.00	3.00	-0.29	-0.33	NO			
	0.10	0.90	-3.00	3.00	-0.37	-0.41	NO			
$ \mu_2 - \mu_1  = 5$	0.50	0.50	-2.50	2.50	0.00	0.00	0.00	-4.97	4.97	NO
	0.45	0.55	-2.50	2.50	-0.04	-0.05	-0.30	-4.68	5.23	NO
	0.40	0.60	-2.50	2.50	-0.08	-0.10	-0.61	-4.37	5.49	NO
	0.35	0.65	-2.50	2.50	-0.12	-0.15	-0.96	-4.01	5.75	NO
	0.30	0.70	-2.50	2.50	-0.17	-0.20	-1.41	-3.56	6.02	NO
	0.25	0.75	-2.50	2.50	-0.22	-0.26	NO			
	0.20	0.80	-2.50	2.50	-0.28	-0.33	NO			
	0.15	0.85	-2.50	2.50	-0.35	-0.41	NO			
	0.10	0.90	-2.50	2.50	-0.44	-0.53	NO			
$ \mu_2 - \mu_1  = 4$	0.50	0.50	-2.00	2.00	0.00	0.00	0.00	-3.89	3.89	NO
	0.45	0.55	-2.00	2.00	-0.05	-0.07	-0.32	-3.62	4.15	NO
	0.40	0.60	-2.00	2.00	-0.10	-0.14	-0.67	-3.28	4.38	NO
	0.35	0.65	-2.00	2.00	-0.15	-0.21	-1.12	-2.85	4.62	NO
	0.30	0.70	-2.00	2.00	-0.21	-0.28	NO			
	0.25	0.75	-2.00	2.00	-0.28	-0.37	NO			
	0.20	0.80	-2.00	2.00	-0.35	-0.47	NO			
	0.15	0.85	-2.00	2.00	-0.43	-0.58	NO			
	0.10	0.90	-2.00	2.00	-0.55	-0.74	NO			
$ \mu_2 - \mu_1  = 3$	0.50	0.50	-1.50	1.50	0.00	0.00	0.00	-2.68	2.68	NO
	0.45	0.55	-1.50	1.50	-0.07	-0.12	-0.50	-2.29	2.97	NO
	0.40	0.60	-1.50	1.50	-0.14	-0.24	NO			
	0.35	0.65	-1.50	1.50	-0.21	-0.38	NO			
	0.30	0.70	-1.50	1.50	-0.28	-0.53	NO			
	0.25	0.75	-1.50	1.50	-0.37	-0.71	NO			
	0.20	0.80	-1.50	1.50	-0.46	-1.50	NO			
	0.15	0.85	-1.50	1.50	-0.58	-1.50	NO			
	0.10	0.90	-1.50	1.50	-0.73	-1.50	NO			

Table 2. Simulation study to compare multi-modality detection methods

Population Density	Dip Test P-value (D)			Silverman Test P-value (S)			BMT
	Mean (D)	Std(D)	% multi-mode	Mean (S)	Std(S)	% multi-mode	% multi-mode
N(0,1)	0.99	0.04	0.00	0.48	0.25	0.00	0.00
Beta(2,4)	0.98	0.04	0.00	0.54	0.28	2.00	0.00
$\{N(-1.1, 1) + N(1.1, 1)\}/2$	0.81	0.22	0.00	0.22	0.21	29.00	69.00
$\{Beta(4, 6) + Beta(7, 3)\}/2$	0.84	0.22	0.00	0.31	0.25	21.00	49.00
$\{N(-2.5, 1) + N(0, 1) + N(2.5, 1)\}/3$	0.10	0.14	52.00	0.03	0.03	79.00	96.00

## 5. SIMULATION STUDY & REAL DATA ILLUSTRATION

Throughout this section we set the BTM threshold to 10% and use the adjustment described in the paragraph above. For details see Algorithm 3 in Appendix C.

### 5.1. Modality Assessment

Testing for homogeneity of a population is an important statistical problem (Aitkin & Rubin, 1985; Müller & Sawitzki, 1991; Roeder, 1994). Here, we use the BMT to detect the presence of two or more dominant modes in the density. We compare its performance with two popular modality assessment procedures: (i) kernel density estimate based test of Silverman (1981) (ii) histogram based Diptest proposed by Hartigan & Hartigan (1985). Larger values of the statistics signify departures from the null hypothesis of unimodality. P-values of the Silverman test are calculated using the R-package referenced in Vollmer et al. (2013). R-packge of Maechler (2013) is used for implementing the Dip test. Further details about these tests are proved in Appendix C.1.

We considered 5 different simulation scenarios, in which 100 independent samples of size 10000 were generated and subjected to modality analysis. In Table 2 we report the percentage of cases in which multi-modality was detected. P-values for the Dip and Silverman tests were computed based on 1000 MCMC simulations, and decision on the null hypothesis of unimodality was made at 5% level of significance. The mean and the standard deviation of the p-values from these tests are also reported. In the two unimodal scenarios we considered, the BMT matched the Silverman and the Dip tests in confirming unimodality of the population distribution with high certainty. In the other three non-unimodal cases, which included normal and beta mixtures, the BMT performed better than the Dip and Silverman test in detecting multi-modality.

### 5.2. Comparisons with number of clusters estimation methods

We study the potency of the BMT in detecting the true number of clusters. We compare its performance with the following *number of clusters* estimation methods: (i) the CH index of Caliński & Harabasz (1974) (ii) the KL index of Krzanowski & Lai (1988) (iii) H measure of Hartigan (1975) (iv) silhouette statistic based KR index of Kaufman & Rousseeuw (2009), and (v) the Gap statistics of Tibshirani et al. (2001). Detailed descriptions of these procedures are provided in Appendix C.2. The number of clusters estimation approaches are further sub-divided into local and global methods (Gordon, 1996). Our method is a local method while the other 5 methods are global methods. In Table 3 we report the performance of our approach, along with the above 5 methods, in detecting the number of clusters in four different simulation scenarios. We consider three univariate and one multivariate (10-dimensional) normal mixtures regimes.

Table 3. Number of clusters detected in 100 trials for four simulation scenarios

True Population Density	Methods	Number of Clusters									
		1	2	3	4	5	6	7	8	9	10+
$0.2 N(-4, 1) + 0.8 N(4, 1)$ Sample Size = 2000	CH	0	<b>1</b>	0	0	0	0	0	0	99	0
	KL	0	<b>1</b>	0	99	0	0	0	0	0	0
	Hartigan	0	<b>1</b>	0	99	0	0	0	0	0	0
	Gap	0	<b>100</b>	0	0	0	0	0	0	0	0
	Silhouette	0	<b>100</b>	0	0	0	0	0	0	0	0
	BMT	0	<b>99</b>	1	0	0	0	0	0	0	0
$0.3 N(-5, 1) + 0.35 N(0, 1) + 0.35 N(5, 1)$ Sample Size = 2000	CH	0	0	<b>0</b>	0	0	0	0	0	0	100
	KL	0	0	<b>0</b>	0	0	0	0	1	0	99
	Hartigan	0	0	<b>100</b>	0	0	0	0	0	0	0
	Gap	0	0	<b>100</b>	0	0	0	0	0	0	0
	Silhouette	0	0	<b>100</b>	0	0	0	0	0	0	0
	BMT	0	0	<b>100</b>	0	0	0	0	0	0	0
$0.3 N(-2.5, 1) + 0.35 N(0, 1) + 0.35 N(2.5, 1)$ Sample Size = 2000	CH	0	0	<b>0</b>	0	0	0	0	0	0	100
	KL	0	0	<b>0</b>	0	0	0	0	1	99	0
	Hartigan	0	0	<b>0</b>	0	0	0	0	1	99	0
	Gap	0	99	<b>0</b>	0	0	0	0	0	0	0
	Silhouette	0	99	<b>0</b>	0	0	0	0	0	0	0
	BMT	0	0	<b>100</b>	0	0	0	0	0	0	0
$\{0.5 N(-1.5, 1) + 0.5 N(1.5, 1)\}$ $\otimes \{0.4 N(-2, 1) + 0.6 N(2, 1)\}$ $\otimes \{N(0, 1)\}^8$ Sample Size = 2000	CH	0	50	50	<b>0</b>	0	0	0	0	0	0
	KL	0	0	50	<b>0</b>	0	0	0	0	0	50
	Hartigan	0	0	50	<b>50</b>	0	0	0	0	0	0
	Gap	0	100	0	<b>0</b>	0	0	0	0	0	0
	Silhouette	0	50	50	<b>0</b>	0	0	0	0	0	0
	BMT	0	0	0	<b>50</b>	0	48	0	0	0	2

100 independent realizations were used for each study and the distribution of the number of clusters detected by the methods are reported. The CH, KL, H, KR and Gap statistics were computed based on  $k$ -means clustering using euclidean distance. The entire sample was used while implementing these methods via the NbClust R-package of Charrad et al. (2014).

In our first univariate example, we consider a highly non-symmetric mixture of two normal densities. Each of them has unit variance and their means are fairly well-separated. We observe that the methods due to CH, KL and Hartigan fail to recover the bimodal structure, but the Gap, Silhouette and BMT successfully detect the two clusters. Next, we considered a tri-modal non-symmetric scenario with well-separated univariate Gaussian mixtures. All the methods other than CH and KL are able to detect the true number of clusters in this example. However, when we half the separation between the adjacent normal means in the above set-up, we observe that all the methods other than the BMT are unable to detect the true number of clusters. The potency of the BMT can be attributed to its effectiveness in truncating the support and zooming in on the troughs of the density. We report this case in our third simulation example. Figure 6 in Appendix C.2 shows the plot of the densities used in these numerical experiments. In our last example, we consider a 10 dimensional dataset, which is generated from a product density. The first two dimensions are generated respectively from a symmetric and a non-symmetric mixture of two-gaussians. The rest eight dimensions just contain white noise. We observe that while all other methods completely fail to detect the four clusters in this product space, the method due to Hartigan and the BMT detect the four clusters with 50% accuracy. However, in the cases where they fail, the method due to Hartigan undercounts, and BMT overcounts, the number of clusters.

## 5.3. Performance on Large Data-sets

In Table 4, we report the performance of the BMT across 4 different simulation examples involving large samples generated from Gaussian mixtures. For each example, 100 independent data sets are generated from the population density and the distribution of the number of clusters detected by BMT is reported (the frequencies are in parenthesis). We also report the average and standard deviations of the Mean Square Errors (MSE) over the cases where the algorithm correctly detects the true number of clusters. The oracle MSE is calculated based on partitions that use the minima of the true population density.

Table 4. Performance of the BMT on simulated datasets of large sample sizes

Population Density	Sample Size	Time in Sec per Replicate	Number of Clusters	MSE		Oracle MSE
				Mean	SD	
$\{N(-2.5, 1) + N(0, 1) + N(2.5, 1)\}/3$	$10^4$	0.70	2 (3), <b>3 (96)</b> , 4 (1)	0.6817	0.0405	0.6564
$0.5 N(-5, 1) + 0.25 N(0, 1) + 0.25 N(5, 1)$	$5 \times 10^4$	11.58	<b>3 (100)</b>	1.1152	0.0125	0.9769
$\{N(-1.1, 1) + N(1.1, 1)\}/2$	$10^5$	44.07	1 (25), <b>2 (70)</b> , 3 (5)	0.6905	0.0258	0.6789
$\{N(0, 1) \pm N(4, 1) \pm N(8, 1)\}/5$	$10^5$	38.98	<b>5 (100)</b>	0.8909	0.0036	0.8909

Over all the four different simulation experiments, we found that the BMT algorithm correctly detected the true number of clusters with high certainty. Also, the average MSE was observed to be very close to the Oracle risk. To demonstrate the scalability of the proposed method, we report the average elapsed time (in Seconds) per replications. The numerical experiments were performed at the Center for High Performance Computing (<http://hpcc.usc.edu>) of the University of Southern California. The computations were done in R version 3.1.1 on Dual Quad-core Intel Xeon 2.33 GHz, 16GB Memory nodes. We used the `snowfall` package of Knaus (2013) to distribute computations over 100 cpus. For each of the simulation setups the algorithm was also executed on an iMac desktop with 2.9 GHz Intel Core i5 processor and 8 GB memory, requiring an approximate run time of 10 seconds, 5 minutes and 20 minutes for 10000, 50000 and 100000 sample sizes, respectively.

## 5.4. Real Data Illustration: Sub-population analysis in Single Cell Virology

We demonstrate an application of our clustering approach in a *single-cell Mass Cytometry* (Bendall et al., 2011) based virology study. We analyze the data reported in Sen et al. (2014), where the effect of Varicella Zoster Virus (VZV) on human tonsil T cell is studied. VZV is a human herpesvirus and causes varicella and zoster (Zerboni et al., 2014). We study protein expressions from five independent experiments, each containing an Uninfected (UN) and a Bystander (BY) populations. Bystanders are cells in the VZV infected population, which are not directly infected by the virus, but are influenced by neighboring virus infected cells. Protein expression values are studied on the arcsinh scale. Non-expressed values are uniformly distributed between  $[-1, 1]$ . Cellular sub-populations are detected by clustering the populations based on the expressions of “core-proteins”, which are associated with T cell activation (Newell et al., 2012). Most of the samples have large sizes, usually on the order of  $\sim 10^5$ . Traditional clustering techniques fail to accommodate such large sample sizes and resort to sub-sampling based approaches (Qiu et al., 2011; Linderman et al., 2012). The BMT, on the other hand, has the advantage of being scalable enough to conduct clustering analysis on the entire sample.

Table 5. *Sizes and Proportions of dominant clusters detected by BMT across 5 independent Virology experiments*

SUB-POPULATIONS	Experiment I		Experiment II		Experiment III		Experiment IV		Experiment V	
	UN	BY	UN	BY	UN	BY	UN	BY	UN	BY
DUAL POSITIVE	8411 (8.8%)	6596 (7.3%)	5253 (5.8%)	4169 (5.7%)	4971 (6.0%)	2703 (5.4%)	3795 (5.0%)	1510 (4.6%)	8047 (8.5%)	5225 (8.0%)
DUAL NEGATIVE	2723 (2.8%)	2973 (3.3%)	3537 (3.9%)	2631 (3.6%)	4433 (5.3%)	2935 (5.9%)	4354 (5.8%)	2196 (6.7%)	5012 (5.3%)	2881 (4.4%)
CD4 NON-NAIVE	7993 (8.4%)	10636 (11.8%)	15144 (16.7%)	11556 (15.9%)	21444 (25.9%)	12429 (25.0%)	22149 (29.7%)	8508 (26.1%)	30034 (31.9%)	20469 (31.3%)
CD4 NAIVE	69977 (73.7%)	64119 (71.1%)	57744 (63.7%)	47374 (65.1%)	45764 (55.3%)	27987 (56.3%)	35458 (47.5%)	16390 (50.4%)	40398 (43.0%)	28524 (43.7%)
CD8 NAIVE	5654 (6.0%)	5671 (6.3%)	8599 (9.5%)	6571 (9.0%)	5798 (7.0%)	3490 (7.0%)	8271 (11.1%)	3774 (11.6%)	9869 (10.5%)	7829 (12.0%)
POPULATION SIZE	94837	90157	90641	72699	82637	49672	74540	32497	93878	65244

The three proteins, CD4, CD8 and CD45RA (naive), classify T cells, for the most part, and are used as core-proteins. For each of the 10 samples (UN and BY from experiments I-V), based on the expressions of the above three proteins, we performed automated clustering by using BMT in the three dimensional space. Figure 7 and 8 in Appendix C-3 show that in all the cases, the BMT detects unimodality for CD4 and CD45RA and bimodality for CD8 expression values. Using the bi-modality of CD8 and the BMT detected splits, we classify cells as CD8-high and CD8-low. Also, considering the expression and non-expressions of the other two markers we simultaneously classify cells into the following clusters: (i) Dual positive: CD4 expressed and CD8 High (ii) Dual-negative: CD4 non-expressed and CD8 low (iii) CD4 Non-Naive: CD4 expressed and CD45RA non-expressed (iv) CD4 Naive: CD4 expressed and CD45RA non-expressed (v) CD8 Naive: CD8 high and CD45RA expressed.

Table 5 shows the sizes and proportional representations of these clusters (sub-populations) across the five experiments. The BMT based sub-populations resemble the T-cell biology based phenotypic classification in Sen et al. (2014). They also revalidate that the sub-population distribution in the Bystander cells is not much different from that of the uninfected, though the UN sub-population distribution varies across experiments. Using this BMT based categorization of the T-cells, sub-population level cell-signaling patterns can be subsequently studied. Figure 9 in Appendix C-3 shows the heatmap of the protein expressions (core + signaling proteins) of the sub-populations from Experiment I.

## 6. DISCUSSION

We present a penalized clustering framework, which is not only consistent, but also scalable to large sample sizes. Our approach shows that fast  $\ell_1$  based convex relaxations of traditional clustering criteria can be used in large data sets with statistical guarantees. Future work on the rates of convergence of the proposed framework will help us investigate the problem of rare clusters detection. Also, following the the lines of Witten & Tibshirani (2010), it would be useful

to incorporate an automated feature selection approach within the convex clustering framework. This would allow us to extend the BMT approach to high dimensional scenarios.

The R code and data sets used for the producing Tables 1-5, can be downloaded from <http://www-bcf.usc.edu/~gourab/code-bmt>. An R package implementing the proposed method will be made available at <http://cran.r-project.org/>.

## 7. ACKNOWLEDGEMENT

Radchenko's research was partially supported by NSF Grant DMS-1209057. Computing resources were provided by the University of Southern California Center for High Performance Computing.

## APPENDIX

### A. DETAILED PROOFS FOR THE RESULTS IN SECTIONS 2-4

#### *Proof of Theorem 1*

Let  $\lambda_0 = 0$ . Suppose that the first merge happens at  $\lambda = \lambda_1$ , the second at  $\lambda = \lambda_2$ , and so on. We will first show that, with probability tending to one, values  $\lambda_k$  form an increasing sequence. Consider two merges,  $C_3 = C_1 \cup C_2$  and  $C = C_3 \cup C_4$ . For concreteness, we will focus on the case where cluster  $C_4$  exists at the time of the first merge, and establish

$$\frac{\bar{X}_{C_2} - \bar{X}_{C_1}}{|C_3|} \leq \frac{\bar{X}_{C_4} - \bar{X}_{C_3}}{|C|}. \quad (\text{A1})$$

This will complete the proof because of the continuity of the underlying distribution. The complementary case, where  $C_4$  is formed after the first merge can be analyzed analogously.

Suppose that the above inequality does not hold. Then, taking into account representation  $|C_3|\bar{X}_{C_3} = |C_1|\bar{X}_{C_1} + |C_2|\bar{X}_{C_2}$ , we can derive

$$\begin{aligned} \bar{X}_{C_4} - \bar{X}_{C_2} &= \bar{X}_{C_4} - \bar{X}_{C_3} - |C_1| \cdot |C_2|^{-1} \cdot (\bar{X}_{C_3} - \bar{X}_{C_1}) \\ &= \bar{X}_{C_4} - \bar{X}_{C_3} - |C_1| \cdot |C_3|^{-1} \cdot (\bar{X}_{C_2} - \bar{X}_{C_1}) \\ &< (\bar{X}_{C_2} - \bar{X}_{C_1}) \left( \frac{|C|}{|C_3|} - \frac{|C_1|}{|C_3|} \right) = \frac{|C_2| + |C_4|}{|C_3|} (\bar{X}_{C_2} - \bar{X}_{C_1}). \end{aligned}$$

The resulting inequality contradicts the merge  $C_3 = C_1 \cup C_2$ .

The KKT conditions for optimization problem (2) are satisfied if there exist  $\beta_{ij}$  with  $|\beta_{ij}| \leq 1$  and  $\beta_{ij} = -\beta_{ji}$ , such that for every  $i$ :

$$\alpha_i - x_i + \lambda \sum_{j \neq i, \alpha_j \neq \alpha_i} \text{sign}(\alpha_i - \alpha_j) + \lambda \sum_{j \neq i, \alpha_j = \alpha_i} \beta_{ij} = 0. \quad (\text{A2})$$

Write  $C(i)$  for the current cluster containing  $x_i$ . Taking into account equations (3), the KKT conditions can be rewritten as follows,

$$\bar{X}_{C(i)} - x_i + \lambda \sum_{j \neq i, j \in C(i)} \beta_{ij} = 0. \quad (\text{A3})$$

We will argue by induction over the number of merges and establish the KKT conditions, (A3), for all  $i$  and for all  $\lambda = \lambda_k$ . If (A3) holds for a particular tuning parameter value  $\lambda_k$ , it also holds for  $\lambda > \lambda_k$ , provided the cluster  $C(i)$  is not modified, if we shrink all the corresponding  $\beta_{ij}$  by a factor of  $\lambda_k/\lambda$ .

For  $\lambda = \lambda_0$ , conditions (A3) hold trivially, with each observation forming its own cluster. Suppose we are able to verify the KKT conditions up to the merge  $k - 1$ . Suppose that the  $k$ -th merge, at  $\lambda = \lambda_k$ , is  $C = C_1 \cup C_2$ . By the discussion above, conditions (A3) hold at  $\lambda = \lambda_k$  for all  $i \notin C$ , and there exist  $\beta_{ij}$

with  $|\beta_{ij}| \leq 1$  and  $\beta_{ij} = -\beta_{ji}$ , such that

$$\overline{X}_{C_1} - x_i + \lambda_k \sum_{j \neq i, j \in C_1} \beta_{ij} = 0 \quad \text{for all } i \in C_1 \quad (\text{A4})$$

$$\overline{X}_{C_2} - x_i + \lambda_k \sum_{j \neq i, j \in C_2} \beta_{ij} = 0 \quad \text{for all } i \in C_2. \quad (\text{A5})$$

We will set  $\beta_{ij} = -1$  for each  $i \in C_1$  and  $j \in C_2$ , and we will keep the remaining  $\beta_{ij}$  values intact. We need to show that

$$\overline{X}_C - x_i + \lambda_k \sum_{j \neq i, j \in C} \beta_{ij} = 0 \quad \text{for all } i \in C. \quad (\text{A6})$$

Consider an  $i \in C_1$ . Equations (A4) imply  $\lambda_k \sum_{j \neq i, j \in C_1} \beta_{ij} = x_i - \overline{X}_{C_1}$ . Recall that  $\lambda_k = (\overline{X}_{C_2} - \overline{X}_{C_1})/|C|$ . It follows that

$$\overline{X}_C - x_i + \lambda_k \sum_{j \neq i, j \in C} \beta_{ij} = \overline{X}_C - \overline{X}_{C_1} + (\overline{X}_{C_1} - \overline{X}_{C_2})|C_2|/|C| = 0, \quad (\text{A7})$$

as required. The argument for  $i \in C_2$  is analogous, but uses equations (A5) instead of (A4).

### *Proof of Theorem 2*

We will prove the result by induction over the number of merges. For each merge we will establish the following claim: the splitting procedure applied to the last formed cluster matches the merging procedure that formed that cluster. It follows that the sequence of clusters formed by the splitting procedure matches the sequence of clusters formed by the merging algorithm.

The claim for merge number one is trivial: the only possible split exactly matches the first merge. Suppose that the claim has been established for the first  $k$  merges. Let  $C$  be the cluster formed by the merge  $k + 1$ , which combines clusters  $C_1$  and  $C_2$ , with  $C_1$  being the left one. It is only left to show that the first splitting procedure applied to  $C$  produces clusters  $C_1$  and  $C_2$ . Consider a possible alternative split:  $C = C_3 \cup C_4$ , with  $C_3$  being the left cluster that is different from  $C_1$ . To verify the claim, we need to establish  $\overline{X}_{C_2} - \overline{X}_{C_1} > \overline{X}_{C_4} - \overline{X}_{C_3}$ . For concreteness, we will focus on the case  $C_3 \subset C_1$ . The case  $C_1 \subset C_3$  can be handled analogously, taking advantage of the inclusion  $C_4 \subset C_2$ .

Define  $C_5 = C_1 \setminus C_3$ . Using representations  $\overline{X}_{C_1} = \overline{X}_{C_3}|C_3|/|C_1| + \overline{X}_{C_5}|C_5|/|C_1|$  and  $\overline{X}_{C_4} = \overline{X}_{C_5}|C_5|/|C_4| + \overline{X}_{C_2}|C_2|/|C_4|$ , we can rewrite the desired inequality as

$$\frac{\overline{X}_{C_2} - \overline{X}_{C_5}}{|C_4|} > \frac{\overline{X}_{C_5} - \overline{X}_{C_3}}{|C_1|}. \quad (\text{A8})$$

Suppose that the cluster  $C_1$  was formed by the merge  $C_{11} \cup C_{12}$ . The induction claim for merges one through  $k$  implies that  $\overline{X}_{C_{12}} - \overline{X}_{C_{11}}$  maximizes the corresponding difference of the averages over all partitions of  $C_1$ . By the monotonicity of the  $\lambda$  values in the merging algorithm, we have  $(\overline{X}_{C_2} - \overline{X}_{C_1})/|C| > (\overline{X}_{C_{12}} - \overline{X}_{C_{11}})/|C_1|$ , which yields

$$\frac{\overline{X}_{C_2} - \overline{X}_{C_1}}{|C|} > \frac{\overline{X}_{C_5} - \overline{X}_{C_3}}{|C_1|}. \quad (\text{A9})$$

Consequently, if we can establish that

$$\frac{\overline{X}_{C_2} - \overline{X}_{C_5}}{|C_4|} > \frac{\overline{X}_{C_2} - \overline{X}_{C_1}}{|C|}, \quad (\text{A10})$$

then the required inequality (A8) is satisfied. Using representation  $\overline{X}_{C_1} = \overline{X}_{C_3}|C_3|/|C_1| + \overline{X}_{C_5}|C_5|/|C_1|$  we can rewrite (A10) as  $(\overline{X}_{C_2} - \overline{X}_{C_1})/|C| > (\overline{X}_{C_5} - \overline{X}_{C_3})/|C_1|$ . The last inequality is true by (A9), which completes the proof.



## Proof of Theorem 3

Define  $A_M = \{(L, R), (L, R) \subseteq D, -M \leq L < R \leq M\}$ . We will need the following lemma, which is proved in the next subsection.

LEMMA A1. For each positive  $M$ ,

$$\sup_{(L,R) \in A_M} \sup_a |\widehat{G}_{L,R}(a) - G_{L,R}(a)| = o_p(1). \quad (\text{A11})$$

Write  $s_n$  for the first split point produced by the sample splitting procedure applied to an interval  $(L, R)$ . Note that  $s_n$  maximizes  $\widehat{G}_{L,R}$ . Define  $\Delta_n = \sup_{A_M} \sup_a |\widehat{G}_{L,R}(a) - G_{L,R}(a)|$ . For all  $(L, R) \in A_M$  we have

$$G_{L,R}(s_n) > \widehat{G}_{L,R}(s_n) - \Delta_n > \max_a G_{L,R}(a) - 2\Delta_n.$$

Lemma A1 gives  $\Delta_n = o_p(1)$ .

If  $D$  is bounded, let  $M = |L_0| \vee |R_0|$ . The argument in the previous paragraph implies that the sample splitting procedure is a  $\delta$ -precision procedure with probability tending to one. Now consider the case of unbounded  $D$ . For concreteness, suppose  $R_0 = \infty$ . Fix a positive  $\delta$  and take  $M = 3\mu_{\delta^{-1}, \infty} + \delta^{-1}$ . By the law of large numbers,  $M - \widehat{\mu}_{\delta^{-1}, \infty} > \widehat{\mu}_{\delta^{-1}, \infty} + \delta^{-1}$ , with probability tending to one. Hence, the following statement holds with probability tending to one. For all intervals  $(L, R)$  with  $R > M$  and  $L \leq \delta^{-1}$ , we have  $\widehat{G}_{L,R}(M) > \sup_{|a| \leq \delta^{-1}} \widehat{G}_{L,R}(a)$ . The last statement implies that when the sample splitting procedure is applied to  $(L, R)$  with  $R > M$ , the split point  $s_n$  satisfies  $|s_n| > \delta^{-1}$ . An analogous argument can be used to handle the case  $L < -M$ .

Consequently, for each positive  $\delta$ , the sample splitting procedure is a  $\delta$ -precision procedure, with probability tending to one. Because the population procedure is continuous, for each positive  $\epsilon$ , the following statement is true with probability tending to one. For each  $\beta \in (\epsilon, \alpha^* - \epsilon)$ , the number of  $\beta$ -splits in the sample procedure is exactly  $k$ . Also, the corresponding split points converge to their population counterparts in probability. Now, take a small enough positive  $\epsilon$  to achieve  $\epsilon < \alpha < \alpha^* - \epsilon$ . By the Glivenko-Cantelli theorem, the difference between the empirical and the population probability of an open interval is  $o_p(1)$ , uniformly over all such intervals. Thus, when the sample splits are thresholded at level  $\alpha$  using the empirical probability, the splits that are retained coincide with those resulting from the thresholding using the population distribution.

## Proof of Lemma A1

Let  $P_n$  denote the empirical measure associated with observations  $x_1, \dots, x_n$ , and let  $P$  be the corresponding population distribution. Standard results from the empirical process theory give us bounds

$$\sup_{l,r} |P_n(l, r) - P(l, r)| = o_p(1) \quad \text{and} \quad \sup_{l,r} \left| \int_l^r x dP_n(x) - \int_l^r x dP(x) \right| = o_p(1). \quad (\text{A12})$$

Fix an arbitrarily small positive  $\epsilon$ . Define  $B_M = \{(l, r), (l, r) \subseteq D, -M \leq l < r \leq M\}$  and  $B_M(\epsilon) = B_M \cap \{(l, r) : r - l \geq \epsilon\}$ . Let  $c = \inf_{B_M(\epsilon)} P(l, r)$ , and note that  $c$  is positive. Using (A12) we can bound  $\sup_{B_M(\epsilon)} |\widehat{\mu}_{l,r} - \mu_{l,r}|$  by

$$\begin{aligned} & \sup_{B_M(\epsilon)} \left| \frac{P_n x(l, r) - P x(l, r)}{P(l, r)} \right| + \sup_{B_M(\epsilon)} |P_n x(l, r)| \left| \frac{1}{P_n(l, r)} - \frac{1}{P(l, r)} \right| \\ & \leq (c\epsilon)^{-1} \sup_{l,r} |P_n x(l, r) - P x(l, r)| + (c\epsilon)^{-1} \frac{\sup_{l,r} |P_n x(l, r)|}{\inf_{B_M(\epsilon)} P_n(l, r)} \sup_{l,r} |P_n(l, r) - P(l, r)| \\ & = (c\epsilon)^{-1} o_p(1) + (c\epsilon)^{-1} \frac{O_p(1)}{c\epsilon + o_p(1)} o_p(1) = o_p(1). \end{aligned}$$

Thus,

$$\sup_{B_M} |\widehat{\mu}_{l,r} - \mu_{l,r}| = \epsilon + \sup_{B_M(\epsilon)} |\widehat{\mu}_{l,r} - \mu_{l,r}| = \epsilon + o_p(1).$$

Because the above stochastic bound holds for every positive  $\epsilon$ , we have  $\sup_{B_M} |\hat{\mu}_{l,r} - \mu_{l,r}| = o_p(1)$ .

*Proof of Corollary 1*

We will need the following result, which is proved in the next subsection.

LEMMA A2. *Suppose that the density,  $f$ , is unimodal. For all  $a, L, R$ , such that  $I_f(L, R) \subseteq D$  and  $L < a < R$ , we have*

$$G_{L,R}(a) < G_{L,R}(L) \vee G_{L,R}(R). \quad (\text{A13})$$

It follows directly from Lemma A2 that the population splitting procedure cannot produce any splits.

Given a positive  $\epsilon$ , there exist positive  $\delta_1$  and  $\tau$ , such that

$$P(-\infty, -\delta_1^{-1}) \vee P(\delta_1^{-1}, \infty) < \epsilon/2 \quad \text{and} \quad \sup_{l \in \mathbb{R}} P(l, l + \tau) < \epsilon/2. \quad (\text{A14})$$

If  $(L, R) \subseteq D$ , then  $G_{L,R}$  can only achieve its maximum at an endpoint, by Lemma A2. Because  $(a, L, R) \mapsto G_{L,R}(a)$  is a continuous function, we can find a positive  $\delta_2$ , such that

$$\min_{-\delta_1^{-1} \leq L \leq R - \tau < R \leq \delta_1^{-1}} \left[ \max_{a \in [L, R]} G_{L,R}(a) - \max_{a \in [L + \tau, R - \tau]} G_{L,R}(a) \right] > \delta_2.$$

Note that  $\max_{a \in [L, R]} G_{L,R}(a)$  is an increasing function of  $R$  and a decreasing function of  $L$ . Thus, if we set  $\delta = \min\{\delta_1, \delta_2\}$ , the above inequality yields

$$\min_{L \leq R - \tau} \left[ \max_{a \in [L, R]} G_{L,R}(a) - \max_{a \in [L + \tau, R - \tau] \cap [-\delta_1^{-1} + \tau, \delta_1^{-1} - \tau]} G_{L,R}(a) \right] > \delta. \quad (\text{A15})$$

Inequality (A15) implies that for any given interval  $(L, R) \subseteq D$ , a  $\delta$ -precision procedure must place the split point in one of the four intervals:  $[L, L + \tau)$ ,  $(R - \tau, R]$ ,  $(-\infty, -\delta_1^{-1} + \tau)$  or  $(\delta_1^{-1} - \tau, \infty)$ . The first interval is only an option if  $L$  is finite, while the second is only an option if  $R$  is finite. Note that such a split does not pass the  $\epsilon$  threshold by inequalities (A14).

Consequently, the population splitting procedure is continuous, and Corollary 1 follows from Theorem 3.

*Proof of Lemma A2*

We will show that for every  $s$  that is an extremum of  $G_{L,R}$  on the interval  $(L, R)$ , we have  $G_{L,R}(s) < G_{L,R}(L) \vee G_{L,R}(R)$ . We will first focus on the case where  $s$  is less than or equal to the mode of the density,  $f$ , restricted to  $(L, R)$ . Direct calculation yields,

$$G'_{L,R}(s) = \frac{f(a)P_{L,R}}{P_{L,s}P_{s,R}} [\mu_{L,s} + \mu_{s,R} - \mu_{L,R} - s]. \quad (\text{A16})$$

Thus, if  $s$  is an extremum, then  $\mu_{s,R} - \mu_{L,R} = s - \mu_{L,s}$  (see Figure 4).

Consequently,

$$\begin{aligned} G_{L,R}(s) &= 2(s - \mu_{L,s}) + \mu_{L,R} - s \\ &< s - L + \mu_{L,R} - s = G_{L,R}(L). \end{aligned}$$

The last inequality follows from the fact that  $f$  is strictly increasing on  $(L, s)$ , which implies  $s - \mu_{L,s} < (s - L)/2$ .

In the case where  $s$  is greater than the mode of  $f$  on  $(L, R)$  we can argue analogously and show that  $G_{L,R}(s) < G_{L,R}(R)$ .

A.1. *Proof of Theorem 4*

We will first show that the population splitting procedure has only one split point, located at  $s^*$ . Consider the following result, which is proved in the next subsection.

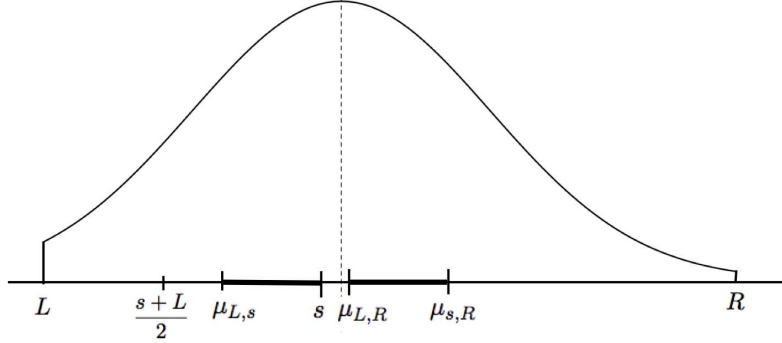


Fig. 4. Illustration of the proof of Lemma 2 on a truncated normal density.

LEMMA A3. Suppose that  $\mu_{L_1, R_1} = (L_1 + R_1)/2$ . If condition (7) holds for all  $L \in [L_1, L_2]$  and  $R \in [R_2, R_1]$ , then  $\mu_{L, R_1} < (L + R_1)/2$  and  $\mu_{L_1, R} > (L_1 + R)/2$  for  $L \in (L_1, L_2]$  and  $R \in [R_2, R_1)$ .

In the proof of Lemma A2 we established that if  $s \in (L, R)$  is a global maximum of  $G_{L, R}$ , then we cannot have either  $\mu_{L, s} > (L + s)/2$  or  $\mu_{s, R} < (s + R)/2$ . Note that  $\mu_{L, s} > (L + s)/2$  for  $s \in [R^*, R_L)$  by Lemma A3. Thus, for  $L < L^*$ , the population procedure applied to  $(L, R_L)$  cannot place a split point in  $[R^*, R_L)$ . An analogous argument shows that there are also no split points in  $(L, L^*]$ . Take a sufficiently large  $M$  to ensure  $(L^*, R^*) \subset (-M, M)$  and  $\mu_{R^*, \infty} - \mu_{-\infty, L^*} < M + \mu_{-\infty, M}$ . Then, if  $(-M, M) \subset (L, R_L)$  and  $s \in (L^*, R^*)$ , we have

$$G_{L, R_L}(s) < \mu_{R^*, \infty} - \mu_{-\infty, L^*} < M + \mu_{-\infty, M} < G_{L, R_L}(L).$$

Consequently,  $\arg \max G_{L, R_L} = \{L, R_L\}$ . Thus, the population splitting procedure will truncate the support of the distribution along  $(L, R_L)$ , until the maximum of  $G_{L, R_L}$  is achieved at an interior point. As mentioned earlier, the proof of Lemma A2 demonstrates that if  $s \in (L, R)$  is a global maximum of  $G_{L, R}$ , then  $\mu_{L, s} \leq (L + s)/2$  and  $\mu_{s, R} \geq (s + R)/2$ . When the above inequalities are equalities, and  $R = R_L$ , we have  $G_{L, R_L}(s) = G_{L, R_L}(L) = G_{L, R_L}(R_L)$ . Thus, the population procedure truncates the support, in a balanced way, along  $(L, R_L)$  down to  $(L^*, R^*)$ , at which point  $G_{L^*, R^*}(s) = G_{L^*, R^*}(L^*) = G_{L^*, R^*}(R^*)$ . Note that for  $L < L^*$  and a sufficiently small positive  $\epsilon$ , Lemma A3 implies  $G_{L+\epsilon, R_L}(L + \epsilon) < G_{L+\epsilon, R_L}(R_L)$  and  $G_{L, R_L-\epsilon}(R_L - \epsilon) < G_{L, R_L-\epsilon}(L)$ , which means that an unbalanced truncation would not be possible. By continuity, when  $\epsilon$  is sufficiently small, condition (7) is also satisfied for  $L \in (L^*, L^* + \epsilon)$  and  $R \in (R^* - \epsilon, R^*)$ . For such  $L$  and  $R$ , Lemma A3 gives  $\mu_{L, s^*} < (L^* + s^*)/2$  and  $\mu_{s^*, R} > (s^* + R^*)/2$ . Consequently, if interval  $(L^*, R^*)$  is truncated, by a small amount, the maximum of  $G$  is no longer achieved at an endpoint. Thus, further truncation of  $(L^*, R^*)$  is not feasible, and the interval is instead split into  $(L^*, s^*)$  and  $(s^*, R^*)$ .

Note that  $f$  restricted to the interval  $(L^*, s^*)$  is unimodal, hence  $(L^*, s^*)$  will not be split any further by Lemma A2. The nature of the asymmetry of the mixture distribution truncated to  $(s^*, R^*)$  implies  $\underline{m} < L^\diamond$  and  $\mu_{L^\diamond, R_{\underline{m}}} < (R_{\underline{m}} + L^\diamond)/2$ . The last inequality continues to hold if  $L^\diamond$  and  $R_{\underline{m}}$  are replaced by larger values. It follows that no split points can be placed in  $[L^\diamond, R^*)$ , as the interval  $(s^*, R^*)$  is being truncated towards  $(\underline{m}, R_{\underline{m}})$ . By Lemma A3,  $\mu_{s, R} < (s + R)/2$  for  $s \in (s^*, L^\diamond)$  and  $R \in [R_{\underline{m}}, R^*]$ . Hence, no split points can be placed in  $(s^*, L^\diamond)$  either. It follows that the interval  $(s^*, R^*)$  will get truncated down to the interval  $(\underline{m}, R_{\underline{m}})$ , on which  $f$  is unimodal. By Lemma A2, there are no more splits.

Using arguments similar to those in the proof of Corollary 1, we can establish that the population splitting procedure is continuous. Theorem 3 then implies the desired properties of the BMT.

#### Proof of Lemma A3

Let  $g(L) = \mu_{L, R_1} - (L + R_1)/2$  and note that  $g(L_1) = 0$ . We will show that  $g'(L) < 0$  for all  $L \in [L_1, L_2]$ , which implies the desired inequality for  $\mu_{L, R_1}$ . The inequality for  $\mu_{L_1, R}$  can be derived using

similar arguments. If  $L \in [L_1, L_2]$  and  $g(L) \leq 0$ , then

$$\begin{aligned} g'(L) &= f(L)(\mu_{L,R_1} - L)/P_{L,R_1} - 1/2 = \frac{f(L)2[\mu_{L,R_1} - L] - P_{L,R_1}}{2P_{L,R_1}} \\ &\leq \frac{f(L)[R_1 - L] - P_{L,R_1}}{2P_{L,R_1}} < 0. \end{aligned}$$

It follows that  $g'(L) < 0$  for all  $L \in [L_1, L_2]$ .

## B. ANALYSIS OF THE POPULATION PROCEDURE FOR GAUSSIAN MIXTURE DISTRIBUTIONS

The dynamics of the population splitting procedure can be analyzed for Gaussian mixture distributions through closed form expressions of  $G_{L,R}$  and its associated functionals. If the population density  $f$  is a mixture of  $k$  normals:  $f(x) := \sum_{i=1}^k w_i \phi(x - \mu_i)$  then using the following inequality,

$$\int x \phi(x - \mu) dx = \mu \Phi(x - \mu) - \phi(x - \mu),$$

we get closed form expressions of  $G_{L,R}$  which can be subsequently optimized:

$$G_{L,R}(a) = P_{a,R}^{-1} \int_a^R x f(x) dx - P_{L,a}^{-1} \int_L^a x f(x) dx \quad \text{where}$$

$$\int_a^R x f(x) dx = \sum_{i=1}^k w_i \mu_i \{ \Phi(R - \mu_i) - \Phi(a - \mu_i) \} - f(R) + f(a),$$

$$\int_L^a x f(x) dx = \sum_{i=1}^k w_i \mu_i \{ \Phi(a - \mu_i) - \Phi(L - \mu_i) \} - f(a) + f(L), \text{ and}$$

$$P_{a,R} = \sum_{i=1}^k w_i \{ \Phi(R - \mu_i) - \Phi(a - \mu_i) \}, \quad P_{L,a} = \sum_{i=1}^k w_i \{ \Phi(a - \mu_i) - \Phi(L - \mu_i) \}.$$

The following alternative expression for  $G_{L,R}(a)$  in terms of the conditional means and density  $f_{L,R}(x) = P_{L,R}^{-1} f(x) \mathbf{I}\{L, R\}$ , where  $\tilde{P}_{a_1, a_2} = P_{L,R}^{-1} P_{a_1, a_2}$ , is also useful:

$$\begin{aligned} G_{L,R}(a) &= \tilde{P}_{L,a}^{-1} \int_a^R x f_{L,R}(x) dx - \tilde{P}_{a,R}^{-1} \int_L^a x f_{L,R}(x) dx \\ &= \{ \tilde{P}_{L,a} \tilde{P}_{a,R} \}^{-1} \left\{ \tilde{P}_{L,a} \mu_{L,R} - \int_{-\infty}^a x f_{L,R}(x) dx \right\} \\ &= f_{L,R}(a) \{ \tilde{P}_{L,a} \tilde{P}_{a,R} \}^{-2} \left[ \mu_{L,R} \tilde{P}_{a,L}^2 + (1 - 2 \tilde{P}_{a,L}) \int_{-\infty}^a x f_{L,R}(x) dx - \tilde{P}_{a,L} \tilde{P}_{a,R} \right]. \end{aligned}$$

Differentiating the above with respect to  $a$ , we arrive at:  $G'_{L,R}(a) = \kappa_{L,R}(a) \times H_{L,R}(a)$ , where

$$\begin{aligned} \kappa_{L,R}(a) &= f(a) P_{L,a}^{-2} P_{a,R}^{-2} P_{L,R}^{-1}, \quad \text{and} \\ H_{L,R}(a) &= \mu_{L,R} P_{L,a}^2 + \{ P_{a,R} - P_{L,a} \} \int_L^a x f(x) dx - a P_{a,L} P_{a,R}. \end{aligned}$$

Note that  $\kappa_{L,R}(a) > 0$  for all  $a \in (L, R)$ . Hence, to track the the extremas of  $G_{L,R}$ , it is enough to search for the zeros of  $H_{L,R}(a)$ . We call  $H_{L,R}$  the normalized  $G'_{L,R}$ . Figure 5 shows the plots of  $G_{L,R}(a)$ , the truncated density and  $H_{L,R}(a)$ , when  $f = 0.35 N(-4, 1) + 0.65 N(4, 1)$ . The plot of  $G_{L,R}$  appears flat in the neighborhood of the split. But, the plot of  $H_{L,R}$  clearly shows only one zero-crossing and demonstrates uniqueness of the maximum of  $G_{L,R}$  in the case of interest.

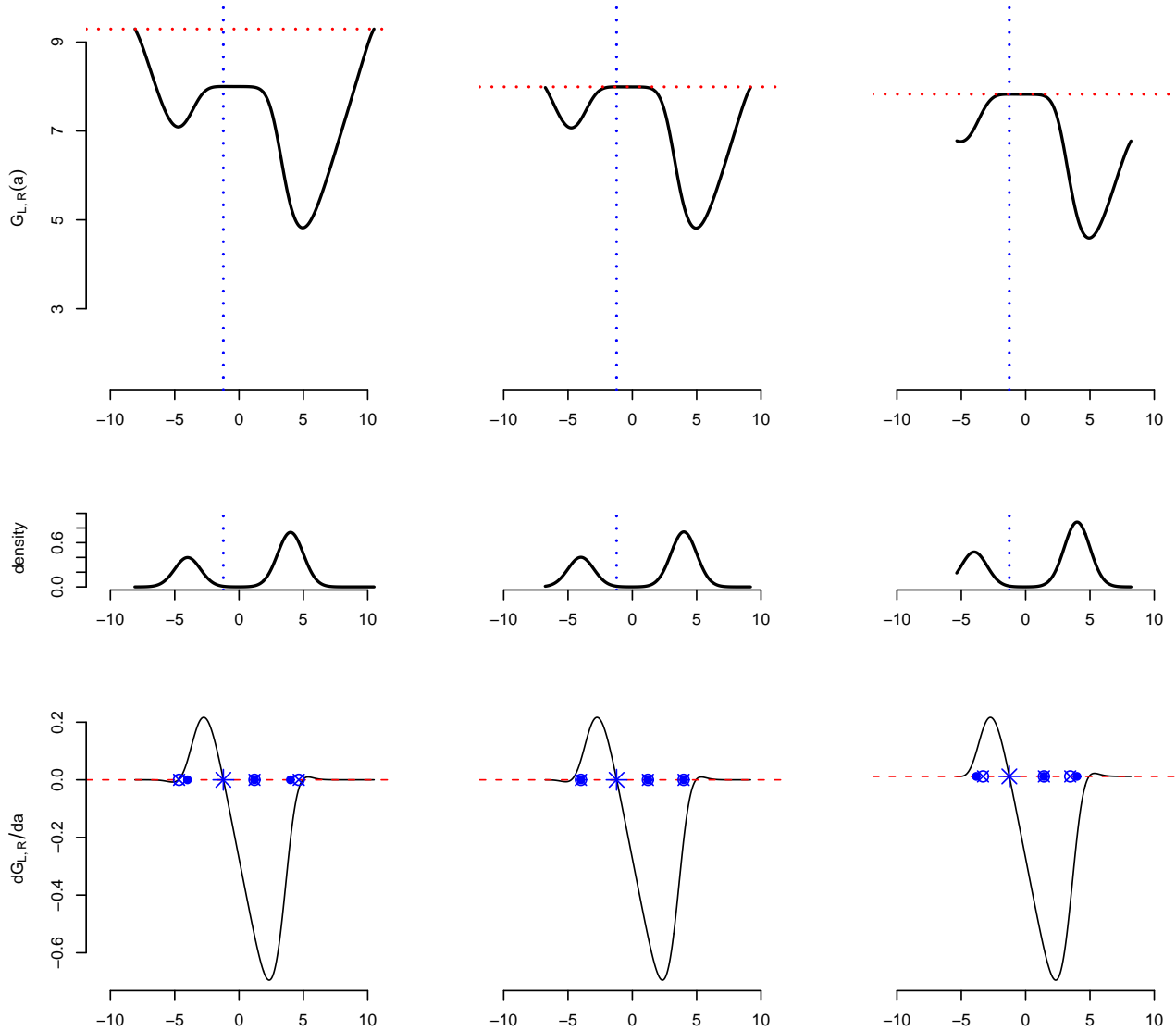


Fig. 5. Across rows we have the plots of  $G_{L,R}(a)$ , the truncated density and the normalized  $G'_{L,R}(a)$ , as  $L$  varies across columns over the 3 cases: (i)  $L < L^*$  (ii)  $L = L^*$  (iii)  $L > L^*$ . The population density used here is  $0.35 N(-4, 1) + 0.65 N(4, 1)$ . The dotted blue line and the stars denote the position of the zero of  $G'$ . In the last row, the conditional means,  $\mu_{Ls}$ ,  $\mu_{LR}$  and  $\mu_{sR}$ , are denoted by circles and the corresponding mid-points,  $(L + s)/2$ ,  $(L + R_L)/2$  and  $(s + R_L)/2$ , by squares. The signs differences  $\delta_1$  and  $\delta_2$ , defined in Section 3, vary as follows (i)  $(\delta_1 > 0, \delta_2 < 0)$  (ii)  $(\delta_1 = 0, \delta_2 = 0)$  (iii)  $(\delta_1 < 0, \delta_2 > 0)$ .

### C. FURTHER DETAILS ON THE SIMULATION STUDY & REAL DATA ILLUSTRATION

For the numerical experiments in Section 5, we implemented the BMT with threshold  $\alpha$  uniformly set at 10%, and with the adjustment of at most 50% truncation for the first split. The details are provided in Algorithm 3.

INITIALIZE:

$K = \text{number of clusters} = n.$

Sort data in ascending order and store them as:  $\mathbf{x} = \{x_1, \dots, x_n\}.$

Assign cluster mean  $\{a_1, a_2, \dots, a_n\}$  to them:  $a_i = x_i$  for  $i = 1, \dots, n.$

Cluster size:  $s_i = 1, i = 1, \dots, n.$

Cluster Membership Indices of  $\mathbf{x}$ :  $I(\mathbf{x}) = \{1, \dots, n\}.$

WHILE  $K > 1$ :

Find the consecutive adjacent centroid distance standardized by cluster sizes:

$$d(j, j+1) \leftarrow (a_{j+1} - a_j) / (s_j + s_{j+1})$$

Find the clusters with minimum merging distance:

$$j^* \leftarrow \arg \min_{1 \leq j \leq K-1} d(j, j+1)$$

Check if it is a Big Merge:  $\min\{s_{j^*}, s_{j^*+1}\} > \lceil n\alpha \rceil$

IF Big Merge: Find and Store *Mass after merge*  $= (s_{j^*} + s_{j^*+1})/n$  and

New Split  $= \{ \max\{\mathbf{x}[I(\mathbf{x}) \text{ is } j^*] s_{j^*} + \min\{\mathbf{x}[I(\mathbf{x}) \text{ is } (j^*+1)]\} s_{j^*+1}\} / (s_{j^*} + s_{j^*+1});$

Merge the  $j^*$  and  $(j^*+1)$  clusters and update the centroid and size of the new cluster:

$$a_{j^*} \leftarrow (s_{j^*} a_{j^*} + s_{j^*+1} a_{j^*+1}) / (s_{j^*} + s_{j^*+1})$$

$$s_{j^*} \leftarrow (s_{j^*} + s_{j^*+1})$$

Reduce the number of clusters in path  $K \leftarrow (K - 1)$

Change cluster indices & cluster member indices of data according to the above reduction:

FOR  $k$  in  $(j^*+1) : K, s_k \leftarrow s_{k+1}; a_k \leftarrow a_{k+1}$

FOR ALL  $I(\mathbf{x}) > j^*$ : reduce index by 1, i.e.,  $I(\mathbf{x}) = I(\mathbf{x}) - 1$

ADJUSTMENT: IF *Mass after merge* in the TOP SPLIT  $< 50\%$ , Stored.Splits = NULL;

OUTPUT Stored Splits.

**Algorithm 3:**  $\alpha$ -thresholded BMT algorithm with truncation adjustment

### C.1. Modality Assessment Methods

We compare the performance of the BMT with the following two popular modality assessment procedures:

**Silverman Test** is based on a kernel density estimate. It uses the idea that if the population density is non-unimodal, a large value of the bandwidth will be required to smooth the data to a unimodal density estimate (Silverman, 1981). The test uses the minimum bandwidth that produces a unimodal kernel estimator. Large values of the minimum bandwidth based test-statistic provide evidence to support the alternative hypothesis of multi-modality. To conduct the Silverman test, we use the R-package referenced in Vollmer et al. (2013) and available from the [http://www.uni-marburg.de/fb12/stoch/forschung/rpackages/silvermantest\\_manual.pdf](http://www.uni-marburg.de/fb12/stoch/forschung/rpackages/silvermantest_manual.pdf). It is based on Gaussian kernels and incorporates Hall & York (2001) adjustment for calculating the p-value.

**The Dip Test** proposed by Hartigan & Hartigan (1985) is a histogram based method, which does not require estimating the density. The Dip-statistic is the minimum Kolmogorov-Smirnov distance between the empirical distribution and the class of unimodal distributions. Larger values of the Dip-statistic signify departure from the null hypothesis of unimodality. P-values are calculated using the R-package of Maechler (2013). The p-value of this test is quite conservative.

C.2. Background: methods for estimating the number of clusters

We compare the performance of BMT with five statistical methods that are popularly used for estimating the number of clusters in a dataset. A comparison study of 30 different approaches in Milligan & Cooper (1985) reports the approach in Caliński & Harabasz (1974) as being one of the best performing global method. It prescribes maximizing the following index over  $k$ :

$$\text{CH}(k) = \frac{B(k)/(k-1)}{W(k)/(n-k)},$$

where  $B(k)$  and  $W(k)$  are respectively the between and the within clusters sum of squares for  $k$  clusters. Another popular approach, due to Krzanowski & Lai (1988), is based on the changes in the within clusters sum of squares as new clusters are formed, and seeks to maximize the following ratio over  $k$ :

$$\text{KL}(k) = \left| \frac{\text{DIFF}(k)}{\text{DIFF}(k+1)} \right| \text{ where } \text{DIFF}(k) = (k-1)^{2/p}W_{k-1} - k^{2/p}W_k.$$

Both these approaches are not defined for  $k = 1$  and can not be used for testing population unimodality. Hartigan (1975) proposed using the smallest  $k$  for which the following ratio of the within cluster sum of squares is greater than 10:

$$\text{H}(k) = \left\{ \frac{W(k)}{W(k+1)} - 1 \right\} / (n - k - 1).$$

It can be used for testing presence of only one cluster. Theoretical thresholds based on the  $F$  distribution can also be used. Gordon (1996) further sub-divides these approaches into local and global methods. Local methods consider individual pairs of clusters and check whether they should be merged. On the other hand, global methods incorporate the entire data in evaluating measures that are subsequently optimized as a function of the number of clusters. Note that BMT is a local method. Along with the above 3 methods, we compare BMT with the following 2 methods.

Given  $k$  clusters, for each data-point  $x_i$  the silhouette statistic of Kaufman & Rousseeuw (2009) uses

- $a(i)$ : the average distance of  $x_i$  to other points in its cluster, and
- $b(i)$ : the average distance of  $x_i$  from points in its nearest neighboring cluster,

and is given by  $\text{sh}_k(i) = (b(i) - a(i))/\max\{a(i), b(i)\}$ . Large values of  $\text{sh}_k(i)$  signify good clustering. A popular estimate of the optimal number of clusters is based on maximizing the average silhouette statistic,

$$\text{KR}(k) = n^{-1} \sum_{i=1}^n \text{sh}_k(i) \quad \text{over } k \geq 2.$$

The Gap statistics of Tibshirani et al. (2001) uses the ‘elbow phenomenon’ (Thorndike, 1953) by estimating the number of clusters at the transition point, where the decline in the within cluster dispersion first slackens. The goodness of clustering for  $k$  clusters is defined as:

$$\text{Gap}_n(k) = \mathbb{E}_n^* \{\log(\tilde{W}(k))\} - \log(\tilde{W}(k)),$$

where  $\tilde{W}(k)$  is the size-normalized intra-cluster sums of squares. The expectation is over reference datasets and can be estimated by the mean of  $\log \tilde{W}^*(k)$  over  $B$  i.i.d. datasets that are generated by sampling uniformly from the original dataset’s range. The standard deviation,  $\text{std}(k)$  of  $\log \tilde{W}^*(k)$ , is also recorded, and an estimate of the optimal number of clusters in the datasets is given by the smallest  $k$  for which the following holds:

$$\text{Gap}(k) \geq \text{Gap}(k+1) - (1 + B^{-1})^{-1/2} \text{std}(k+1).$$

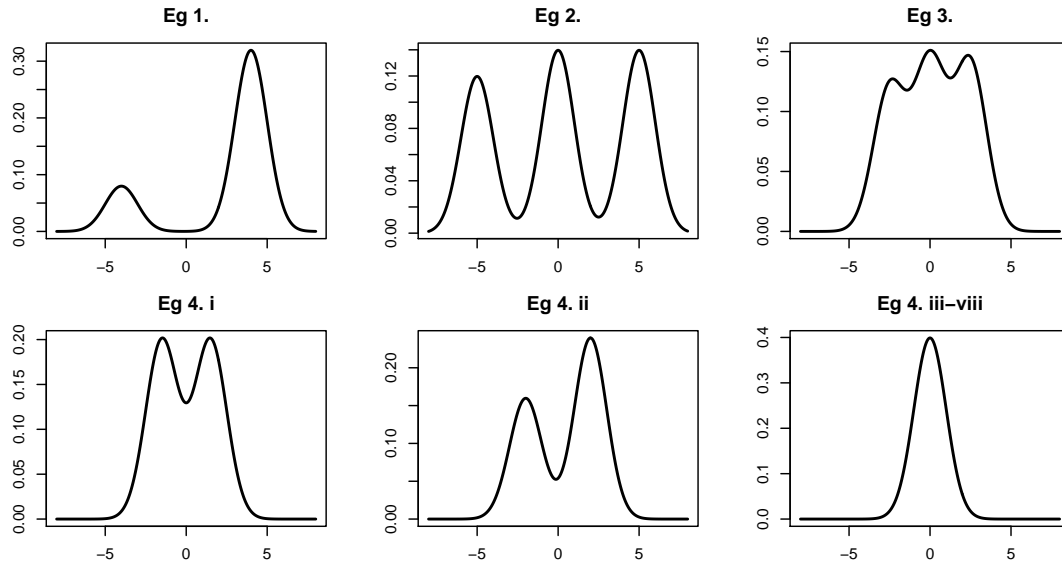


Fig. 6. Plot of the univariate densities used in the different numerical experiments of Table 3

### C.3. BMT & Sub-population Analysis in Single Cell Virology

We demonstrate an application of our clustering method in an immunology study conducted at single cell level. Emerging technologies (Wang & Bodivitz, 2011) have recently enabled us to collect proteomic data sets at single cell resolution. These data sets reflect the variations of protein expressions across cells and need clustering techniques for detection of cellular sub-populations. Typically, sub-populations are detected by core-protein expressions based cluster analysis of the samples, and the signaling expressions of the resultant sub-populations are subsequently studied. In Figures 7 and 8 we display the results of the BMT induced clustering on the virology datasets of Sen et al. (2014). Figure 9 shows the post-clustering, sub-population level signaling expressions.



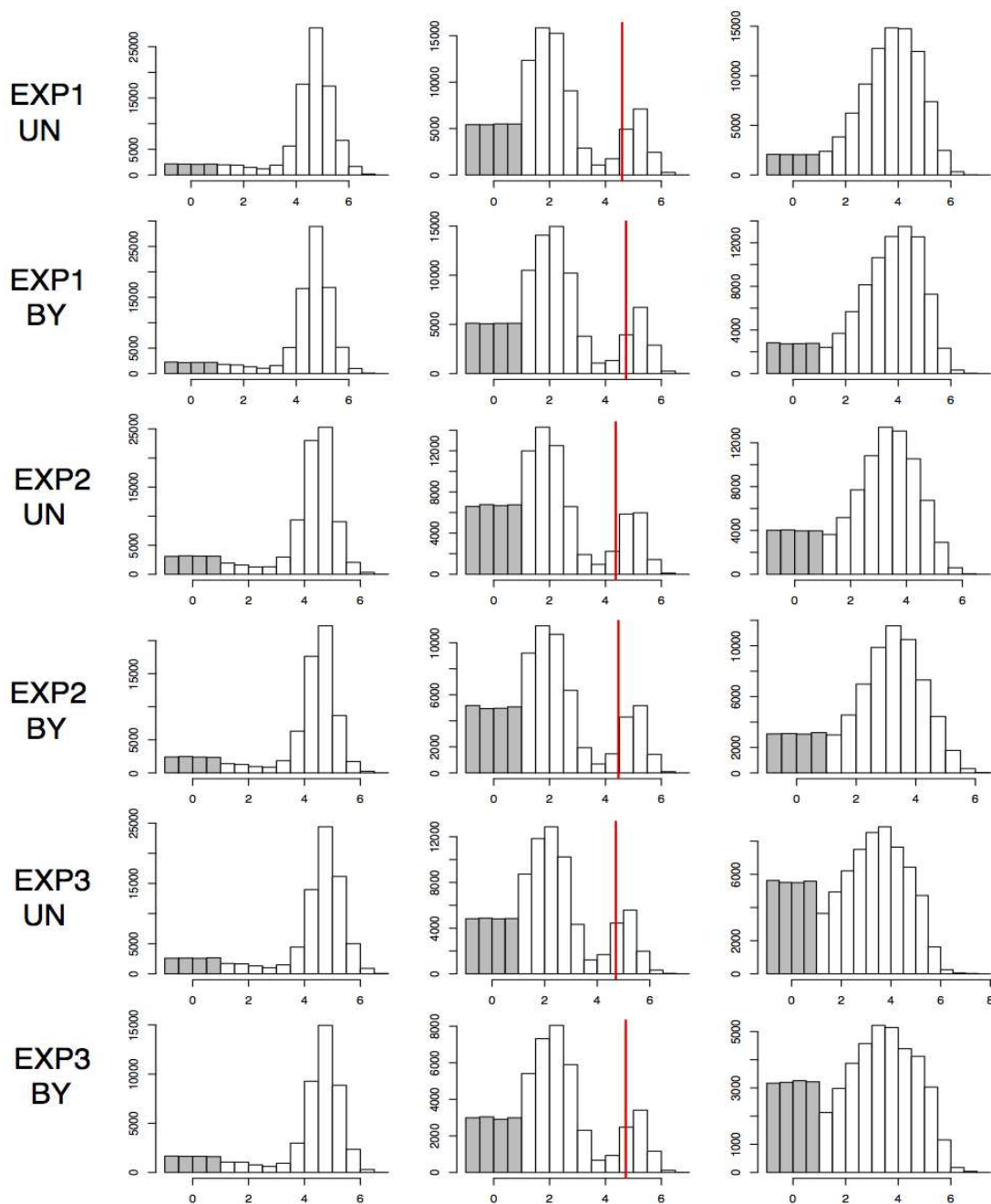


Fig. 7. Across columns we have histograms of the expression values of the proteins CD4, CD8 and CD45RA, respectively. Along rows, from top to bottom, we have the histograms of the Uninfected and Bystander population, respectively, for the independent experiments I-III. The shaded gray region denotes unexpressed values. Splits in the expression values (if any) detected by BMT are shown by vertical red lines.

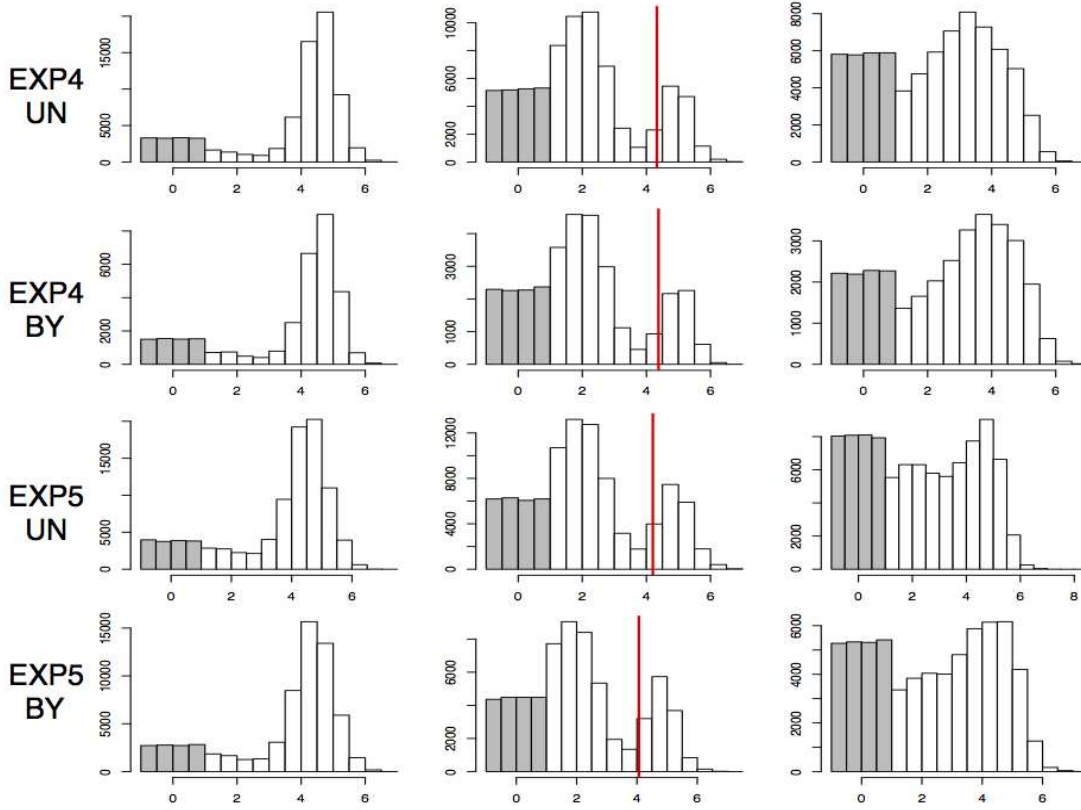


Fig. 8. Across columns we have histograms of the expression values of CD4, CD8 and CD45RA. Across rows are the histograms of UN and BY populations for Experiments IV-V. Splits detected by BMT (if any) are shown by red lines.

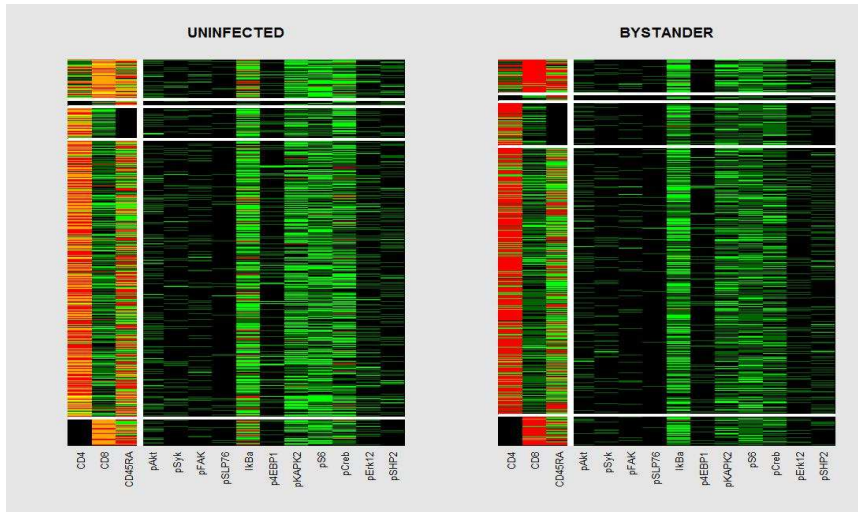


Fig. 9. The above plot shows the heatmaps of the protein expression values (in order of decreasing intensity: Red, Yellow, Green and Black) of the Uninfected and Bystander populations in Experiment I. The horizontal white lines demarcate the five major sub-population detected by BMT algorithm, based on the expression of the three surface markers on the left of the vertical white line. The proteins on the right of the vertical line are associated with cell-signaling. The heatmaps are standardized separately for the two populations.

## REFERENCES

- AITKIN, M. & RUBIN, D. B. (1985). Estimation and hypothesis testing in finite mixture models. *Journal of the Royal Statistical Society. Series B (Methodological)*, 67–75.
- BACH, F. R. & HARCHAOU, Z. (2008). Diffrac: a discriminative and flexible framework for clustering. In *Advances in Neural Information Processing Systems*.
- BENDALL, S. C., SIMONDS, E. F., QIU, P., AMIR, E., KRUTZIK, P. O., FINCK, R., BRUGGNER, R. V., MELAMED, R., TREJO, A., ORNATSKY, O. I., BALDERAS, R. S., PLEVritis, S. K., SACHS, K., PE'ER, D., TANNER, S. D. & NOLAN, G. P. (2011). Single-cell mass cytometry of differential immune and drug responses across a human hematopoietic continuum. *Science (New York, N.Y.)* **332**, 687–696.
- BONDELL, H. D. & REICH, B. J. (2008). Simultaneous regression shrinkage, variable selection, and supervised clustering of predictors with oscar. *Biometrics* **64**, 115–123.
- CALIŃSKI, T. & HARABASZ, J. (1974). A dendrite method for cluster analysis. *Communications in Statistics-theory and Methods* **3**, 1–27.
- CHARRAD, M., GHAZZALI, N., BOITEAU, V. & NIKNAFS, A. (2014). NbClust: An R package for determining the relevant number of clusters in a data set. *Journal of Statistical Software* **61**, 1–36.
- CHEN, S. S., DONOHO, D. L. & SAUNDERS, M. A. (1998). Atomic decomposition by basis pursuit. *SIAM journal on scientific computing* **20**, 33–61.
- CHI, E. C. & LANGE, K. (2013). Splitting methods for convex clustering. *arXiv preprint arXiv:1304.0499*.
- GORDON, A. D. (1996). Null models in cluster validation. In *From data to knowledge*. Springer, pp. 32–44.
- HALL, P. & YORK, M. (2001). On the calibration of silverman's test for multimodality. *Statistica Sinica* **11**, 515–536.
- HARTIGAN, J. (1978). Asymptotic distributions for clustering criteria. *The Annals of Statistics*, 117–131.
- HARTIGAN, J. A. (1975). *Clustering algorithms*. Wiley.
- HARTIGAN, J. A. & HARTIGAN, P. (1985). The dip test of unimodality. *The Annals of Statistics*, 70–84.
- HOCKING, T., VERT, J.-P., BACH, F. & JOULIN, A. (2011). Clusterpath: an algorithm for clustering using convex fusion penalties. In *ICML*, L. Getoor & T. Scheffer, eds. Omnipress.
- HOEFLING, H. (2010). A path algorithm for the fused lasso signal approximator. *Journal of Computational and Graphical Statistics* **19**, 984–1006.
- JAIN, A. K. (2010). Data clustering: 50 years beyond k-means. *Pattern Recognition Letters* **31**, 651–666.
- KAUFMAN, L. & ROUSSEEUW, P. J. (2009). *Finding groups in data: an introduction to cluster analysis*, vol. 344. John Wiley & Sons.
- KE, T., FAN, J. & WU, Y. (2013). Homogeneity in regression. *arXiv preprint arXiv:1303.7409*.
- KNAUS, J. (2013). *snowfall: Easier cluster computing (based on snow)*. R package version 1.84-6.
- KRZANOWSKI, W. J. & LAI, Y. (1988). A criterion for determining the number of groups in a data set using sum-of-squares clustering. *Biometrics*, 23–34.
- LINDERMAN, M. D., BJORNSON, Z., SIMONDS, E. F., QIU, P., BRUGGNER, R. V., SHEODE, K., MENG, T. H., PLEVritis, S. K. & NOLAN, G. P. (2012). Cytospade: high-performance analysis and visualization of high-dimensional cytometry data. *Bioinformatics* **28**, 2400–2401.
- MACQUEEN, J. et al. (1967). Some methods for classification and analysis of multivariate observations. In *Proceedings of the fifth Berkeley symposium on mathematical statistics and probability*, vol. 1. California, USA.
- MAECHLER, M. (2013). *dipTest: Hartigan's dip test statistic for unimodality - corrected code*. R package version 0.75-5.
- MILLIGAN, G. W. & COOPER, M. C. (1985). An examination of procedures for determining the number of clusters in a data set. *Psychometrika* **50**, 159–179.
- MÜLLER, D. W. & SAWITZKI, G. (1991). Excess mass estimates and tests for multimodality. *Journal of the American Statistical Association* **86**, 738–746.
- NEWELL, E., SIGAL, N., BENDALL, S., NOLAN, G. & DAVIS, M. (2012). Cytometry by time-of-flight shows combinatorial cytokine expression and virus-specific cell niches within a continuum of cd8+ t cell phenotypes. *Immunity* **36**, 142 – 152.
- POLLARD, D. (1981). Strong consistency of  $k$ -means clustering. *The Annals of Statistics* **9**, 135–140.
- POLLARD, D. (1982). A central limit theorem for  $k$ -means clustering. *The Annals of Probability*, 919–926.
- QIU, P., SIMONDS, E. F., BENDALL, S. C., JR., K. D. G., BRUGGNER, R. V., LINDERMAN, M. D., SACHS, K., NOLAN, G. P. & PLEVritis, S. K. (2011). Extracting a cellular hierarchy from high-dimensional cytometry data with spade. *Nature Biotechnology*.
- RINALDO, A. et al. (2009). Properties and refinements of the fused lasso. *The Annals of Statistics* **37**, 2922–2952.
- ROEDER, K. (1994). A graphical technique for determining the number of components in a mixture of normals. *Journal of the American Statistical Association* **89**, 487–495.
- SEN, N., MUKHERJEE, G., SEN, A., BENDALL, S., SUNG, P., NOLAN, G. & ARVIN, A. (2014). Single-cell mass cytometry analysis of human tonsil t cell remodeling by varicella zoster virus. *Cell Reports* **8**, 633 – 645.
- SHEN, X. & HUANG, H.-C. (2010). Grouping pursuit through a regularization solution surface. *Journal of the American Statistical Association* **105**.

- SHEN, X., HUANG, H.-C. & PAN, W. (2012). Simultaneous supervised clustering and feature selection over a graph. *Biometrika* **99**, 899–914.
- SILVERMAN, B. W. (1981). Using kernel density estimates to investigate multimodality. *Journal of the Royal Statistical Society. Series B (Methodological)*, 97–99.
- SOLTANOLKOTABI, M. & CANDÉS, E. J. (2012). A geometric analysis of subspace clustering with outliers. *Ann. Statist.* **40**, 2195–2238.
- THORNDIKE, R. L. (1953). Who belongs in the family? *Psychometrika* **18**, 267–276.
- TIBSHIRANI, R. (1996). Regression shrinkage and selection via the lasso. *Journal of the Royal Statistical Society. Series B (Methodological)*, 267–288.
- TIBSHIRANI, R. (2011). Regression shrinkage and selection via the lasso: a retrospective. *Journal of the Royal Statistical Society: Series B (Statistical Methodology)* **73**, 273–282.
- TIBSHIRANI, R., SAUNDERS, M., ROSSET, S., ZHU, J. & KNIGHT, K. (2005). Sparsity and smoothness via the fused lasso. *Journal of the Royal Statistical Society: Series B (Statistical Methodology)* **67**, 91–108.
- TIBSHIRANI, R. & WALTHER, G. (2005). Cluster validation by prediction strength. *Journal of Computational and Graphical Statistics* **14**, 511–528.
- TIBSHIRANI, R., WALTHER, G. & HASTIE, T. (2001). Estimating the number of clusters in a data set via the gap statistic. *Journal of the Royal Statistical Society: Series B (Statistical Methodology)* **63**, 411–423.
- TIBSHIRANI, R. J. (2013). Adaptive piecewise polynomial estimation via trend filtering. *arXiv preprint arXiv:1304.2986*.
- VOLLMER, S., HOLZMANN, H. & SCHWAIGER, F. (2013). Peaks vs components. *Review of Development Economics* **17**, 352–364.
- WANG, D. J. & BODIVITZ, S. (2011). Single cell analysis: the new frontier in omics. *Nature Methods*.
- WITTEN, D. M. & TIBSHIRANI, R. (2010). A framework for feature selection in clustering. *Journal of the American Statistical Association* **105**.
- XU, L., NEUFELD, J., LARSON, B. & SCHURMANS, D. (2004). Maximum margin clustering. In *Advances in neural information processing systems*.
- YUAN, M. & LIN, Y. (2006). Model selection and estimation in regression with grouped variables. *Journal of the Royal Statistical Society: Series B (Statistical Methodology)* **68**, 49–67.
- ZERBONI, L., SEN, N., OLIVER, S. L. & ARVIN, A. M. (2014). Molecular mechanisms of varicella zoster virus pathogenesis. *Nature Reviews Microbiology*.